

RACE-OC project: rotation and variability in the open cluster M 11 (NGC 6705)^{*,**}

S. Messina¹, P. Parihar², J.-R. Koo³, S.-L. Kim³, S.-C. Rey⁴, and C.-U. Lee³

¹ INAF - Catania Astrophysical Observatory, via S. Sofia 78, 95123 Catania, Italy
e-mail: sergio.messina@oact.inaf.it

² Indian Institute of Astrophysics, Block II, Koramangala, Bangalore India, 560034, India
e-mail: psp@iiap.res.in

³ Korea Astronomy and Space Science Institute, Daejeon, Korea
e-mail: koojr@kasi.re.kr; slkim@kasi.re.kr

⁴ Department of Astronomy and Space Science, Chungnam National University, Daejeon, Korea

Received 22 April 2009 / Accepted 15 December 2009

ABSTRACT

Context. Rotation and magnetic activity are intimately linked in main-sequence stars of G or later spectral types. The presence and level of magnetic activity depend on stellar rotation, and rotation itself is strongly influenced by the strength and topology of the magnetic fields. Open clusters represent especially useful targets for investigating the connection among rotation, activity, and age. Over time, stellar activity and rotation evolve, providing us with a promising diagnostic tool to determine the age of the field stars.

Aims. The open cluster M11 has been studied as a part of the RACE-OC project (Rotation and ACTivity Evolution in Open Clusters), which aims to explore the evolution of rotation and magnetic activity in the late-type members of open clusters with different ages.

Methods. Photometric observations of the open cluster M 11 were carried out in June 2004 using the LOAO 1 m telescope. The rotation periods of the cluster members were determined by Fourier analysis of photometric data time series. We investigated the relations between the surface activity, characterized by the light curve amplitude, and rotation.

Results. We have discovered a total of 75 periodic variables in the M 11 FoV, of which 38 are candidate cluster members. Specifically, among cluster members we discovered 6 early-type periodic variables, 2 eclipsing binaries, and 30 bona-fide single periodic late-type variables. Considering the rotation periods of 16 G-type members of the almost coeval 200-Myr M 34 cluster, we could determine the rotation period distribution from a more numerous sample of 46 single G stars at an age of about 200-230 Myr and determine a median rotation period of $P = 4.8$ d.

Conclusions. A comparison with the younger M 35 cluster (~150 Myr) and with the older M37 cluster (~550 Myr) shows that G stars rotate more slowly than younger M 35 stars and more rapidly than older M 37 stars. The measured variation in the median rotation period is consistent with the scenario of rotational braking of main-sequence spotted stars as they age. Finally, G-type M11 members have a level of photospheric magnetic activity, as measured by light curve amplitude, comparable to what is observed in the younger 110-Myr Pleiades stars of similar mass and rotation.

Key words. stars: activity – stars: late-type – stars: rotation – starspots – open clusters and associations: general – open clusters and associations: individual: M11

1. Introduction

RACE-OC, which stands for Rotation and ACTivity Evolution in Open Clusters, is a long-term project to study stellar rotation, magnetic activity, and their evolution in the late-type members of open clusters (Messina 2007; Messina et al. 2008). The project's targets are open clusters that, unlike field stars, provide us with a sample of stars spanning a range of masses with the same age, initial chemical composition, environmental conditions, and interstellar reddening. Such stellar samples allow us to accurately investigate the relationships among rotation, activity, and age and their mass dependence.

Indeed, rotation is one basic property of late-type stars. It undergoes dramatic changes in stellar life, as shown by observational studies and also predicted by evolutionary models of angular momentum (Kawaler 1988; MacGregor & Brenner 1991; Krishnamurthi et al. 1997; Bouvier et al. 1997; Sills et al. 2000; Ivanova & Taam 2003; Holzwarth & Jardine 2007). On one hand, the properties of magnetic fields depend on rotation and mass; on the other, they play a fundamental role in altering the rotational properties of late-type stars. For example, they are responsible for the angular momentum loss and for the coupling mechanisms between the radiative core and the external convection zone (e.g., Barnes 2003). This interplay between rotation and magnetic fields provides us with a powerful tool for probing internal stellar structure.

A number of valuable ongoing projects (MONITOR, Hodgkin et al. 2006; EXPLORE/OC, EXtrasolar PLANet Occultation REsearch, von Braun et al. 2005; RCT, Robotically Controlled Telescope project, Guinan et al. 2003) are rapidly increasing our knowledge of the rotational properties of the

* Data corresponding to Figs. 10–25 are only available in electronic form at the CDS via anonymous ftp to cdsarc.u-strasbg.fr (130.79.128.5) or via <http://cdsweb.u-strasbg.fr/cgi-bin/qcat?J/A+A/513/A29>

** Figures 10–25 are only available in electronic form at <http://www.aanda.org>

late-type members of open clusters. However, the sequence of ages at which the angular momentum evolution has been studied still has significant gaps, and the sample of periodic cluster members is not as complete as needed to fully constrain the various models proposed to describe the driving mechanisms of angular momentum evolution.

We have selected open clusters (Messina 2007) and young associations (Messina et al. 2010) with an age in the range from 1 to 500 Myr and, generally, with no earlier rotation and magnetic activity studies. Top priority was given to the open clusters that fill the gaps in the empirical description of the relationships among rotation, activity, and age. We also selected a few extensively studied clusters, such as the Pleiades and the Orion Nebula Cluster (Parihar et al. 2009). The motivation is to make repeated observations over several years to enrich the sample of periodic variables and to explore the long-term magnetic activity, e.g., to search for activity cycles and surface differential rotation (SDR). Our sample also includes open clusters that were previously monitored with different scientific motivations. Analyzing again these archived data time series can provide valuable results in the context of the RACE-OC project. That was the case for M37 (Messina et al. 2008, hereinafter Paper I). Although it was initially observed to search for early-type pulsating variables (Kang et al. 2007), its data time series allowed us to determine, for the first time, the rotational period distribution of G stars at an age of about 550 Myr. Similarly, the M 11 photometric data time series collected with the same goal (Koo et al. 2007), have allowed us to determine the rotational period distribution of G stars at an age of about 230 Myr, again for the first time.

M 11 (NGC 6705; $RA_{J2000.0} = 18 : 51 : 04$, $Dec_{J2000.0} = -06:16:30$) is a ~ 230 Myr intermediate-age open cluster at a distance of nearly $d = 2.0$ kpc, $(m - M) = 12.69 \pm 0.1$. The cluster is subjected to substantial reddening $E(B - V) = 0.428$ mag because of low galactic latitude ($b = -2.8^\circ$). It contains thousands of members within an estimated radius of 16 arcmin. Gonzalez & Wallerstein (2000) found a small metal excess, $+0.10$ dex, in agreement with the general trend to increasing metallicity with decreasing distance from the Galactic center. In the following analysis we adopt the cluster parameters derived by Sung et al. (1999).

The first comprehensive variability study of M 11 was carried out in 2002–2003 by Hargis et al. (2005) in the R band and on a $13.7' \times 13.7'$ field of view. They discovered 39 variables, and they could determine the periodicity for 32 of these. Among late-type stars ($B - V > 0.55$), Hargis et al. (2005) could only identify 15 periodic eclipsing binaries, probably because of the large amplitude of light variation, but no periodic single stars. The poor seeing (~ 5 arc-sec), the use of a small telescope, and the faintness of the cluster's late-type members at a distance of about 2 kpc did not allow them to acquire precise enough data required to detect very low-amplitude variation due to spots. A second comprehensive variability study of M 11 was carried out in 2004 by Koo et al. (2007), who detected all the variables previously found by Hargis et al. (2005) and 43 new periodic variables. Among late-type stars, they discovered 12 W UMa and 2 detached eclipsing binaries. Again, they did not report the discovery of any late-type, low-amplitude periodic single stars, because their study was focused on early-type pulsating variables.

Our investigation, which is based on the Koo et al. (2007) database, aims at detecting the periodicity of the low-amplitude, late-type single members of M 11. In Sect. 2 we give details on observations and data analysis. The rotation period search is presented in Sect. 3 and the results in Sect. 4. Discussion and conclusions are given in Sects. 5 and 6.

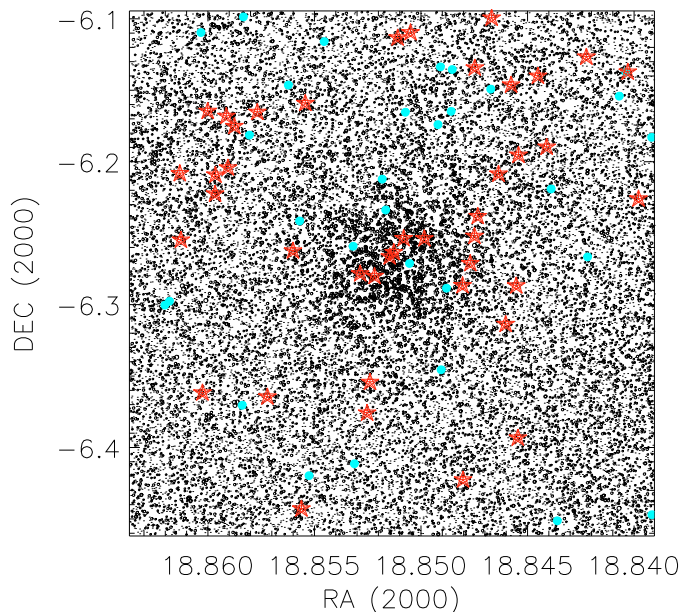


Fig. 1. M 11 field of view ($22.2' \times 22.2'$). The newly discovered and previously known periodic variables are plotted as large red stars and light-blue bullets, respectively

2. Observations and data analysis

The present study is based on observations taken in June 2004 with the 1.0 m telescope at the Mt. Lemmon Optical Astronomy Observatory (LOAO) in Arizona (USA), which feeds a $2K \times 2K$ CCD camera. The observed field of view (FoV) is about $22.2' \times 22.2'$ (see Fig. 1) at the $f/7.5$ Cassegrain focus. We collected a sequence of 406 long- (600 s) and 595 short-exposed (60 s) images in the V -band filter over a total time interval of 18 days. Additional observations in the B bandpass filter were made on one night of October 2004, in order to construct a V vs. $B - V$ color-magnitude diagram. A detailed description of these observations and data reduction can be found in Koo et al. (2007) and Kim et al. (2001).

We detected about 33 400 stars in the $12 < V < 20$ magnitude range in the 600-s long exposures. Their coordinates and the B and V magnitudes are available in the WEBDA open cluster database¹. These stars are represented in Fig. 1 with open circles, whereas the symbol size is proportional to the star's brightness. The overplotted large red stars and light-blue bullets represent the newly discovered and already known periodic variables in the FoV under analysis.

Before analyzing our magnitude time series for the rotation period search, we carefully eliminated possible outliers. First we disregarded all data points that deviated more than 4 standard deviations from the mean of the whole series data. Such a broad limit was adopted to include the light minima of possible eclipsing binaries. In fact, from earlier studies we are aware that there are numerous eclipsing binaries in our FoV. Then, we computed a filtered version of the light curve by means of a sliding median boxcar filter with a boxcar extension equal to 1 h. This filtered light curve was subtracted from the original light curve, and all the points deviating more than 3 standard deviations of the residuals were discarded. Finally, we computed normal points by binning the data on time intervals having the duration of about 1 h,

¹ http://www.univie.ac.at/webda/archive_ngc.html

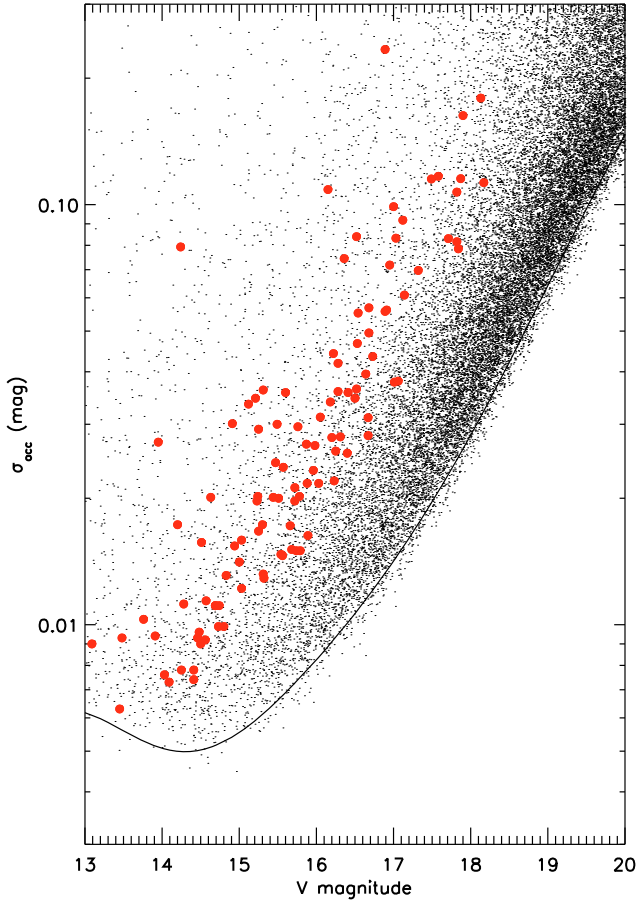


Fig. 2. Photometric accuracy σ_{acc} vs. mean magnitude for the stars in the M 11 FoV. The solid line represents a polynomial fit to the distribution lower envelope. Small red bullets represent the periodic variable stars.

getting a light curve consisting of about 100 normal points on average. Each normal point was obtained by averaging about 4 consecutive frames collected within a time interval of 1 h. We adopted the average standard deviation of our normal points σ_{acc} as photometric accuracy of our observations, rather than the values computed by DAOPHOT while extracting the PSF magnitudes. This standard deviation σ_{acc} is an empirical estimate of the effective precision of our photometry. It represents a conservative value because the true observational accuracy could be, in principle, even better for stars showing substantial variability within the timescale closer to our fixed binning time interval. In Fig. 2 we plot σ_{acc} of the stars in the $13.0 < V < 20.0$ mag range vs. their mean V magnitude. The lower envelope of the σ_{acc} distribution is populated by non variable and variable stars with the least intrinsic variation. Such a lower envelope gives a measure of the best photometric accuracy we achieved at different magnitudes. To construct the relation between observational accuracy and magnitude, we fitted a multi-order polynomial function to the lower σ_{acc} boundary.

The 600-s long exposures have allowed us to achieve a photometric accuracy σ_{acc} in the V band of about 0.006 mag in the $13 < V < 16$ mag range, and better than 0.02 mag for all stars in the magnitude range $16.0 < V < 18$.

The photometric accuracy is slightly poorer than the accuracy we achieved for M 37 (Paper I), although we used the same telescope, instrumental setup, and reduction procedure. M 11 has a distance modulus about 1 mag larger than M 37, and it

is very rich, crowded, and younger than M 37. For example, our candidate periodic stars have on average 2 closeby stars within 5 arcsec and with a brightness difference down to 3 mag. However, we adopted the PSF photometry, which is the most accurate approach to determining the star’s magnitude in crowded fields and which should eliminate any spurious flux contribution from closeby stars. Therefore, we suspect that the slightly poorer photometric accuracy of M 11 with respect to M 37 arises from its younger age and, specifically, from the higher level of short-scale (< 1 h) intrinsic variability.

3. Rotation period search

We used the Scargle-Press method to search for significant periodicities related to the stellar rotation in our data time series. In the following subsections we briefly describe our procedures to identify the periodic variables. The period search was carried out on the 1-h binned data time series, that is, on about 100 data points with respect to the original series of about 400 frames, and after discarding evident outliers, as discussed in the previous section.

3.1. Scargle-Press periodogram

The Scargle technique has been developed to search for significant periodicities in unevenly sampled data (Scargle 1982; Horne & Baliunas 1986). The algorithm calculates the normalized power $P_N(\omega)$ for a given angular frequency $\omega = 2\pi\nu$. The highest peaks in the calculated power spectrum (periodogram) correspond to the candidate periodicities in the analyzed data time series. To determine the significance level of any candidate periodic signal, the height of the corresponding power peak is related to a false alarm probability (FAP), which is the probability that a peak of given height simply stems from statistical variations, i.e. from Gaussian noise. This method assumes that each observed data point is independent of the others. However, this is not strictly true for our data time series that consists of data consecutively collected in the same night and with a much shorter time sampling than both the periodic or the irregular intrinsic variability timescales we are looking for ($P^d = 0.1-15$). The impact of this correlation on the period determination has been highlighted by, e.g., Herbst & Wittenmyer (1996), Stassun et al. (1999), Rebull (2001), Lamm et al. (2004). To overcome this problem, we decided to determine the FAP in different way than proposed by Scargle (1982) and Horne & Baliunas (1986), where the latter is only based on the number of independent frequencies.

3.2. False alarm probability

Following the approach outlined by Herbst et al. (2002), randomized time series data sets were created by randomly scrambling the day number of the Julian day while keeping photometric magnitudes and the decimal part of the JD unchanged. This method preserves any correlation that exists in the original data set. We noticed that, to produce the simulated light curves, Lamm et al. (2004) randomized the observed magnitudes instead of the epochs of observation. Then, we applied the periodogram analysis to about 10 000 “randomized” data time series for each star. We retained the highest power peak and the corresponding period of each computed periodogram. The FAP related to a given power P_N is taken as the fraction of randomized light curves that have the highest power peak exceeding P_N , which in

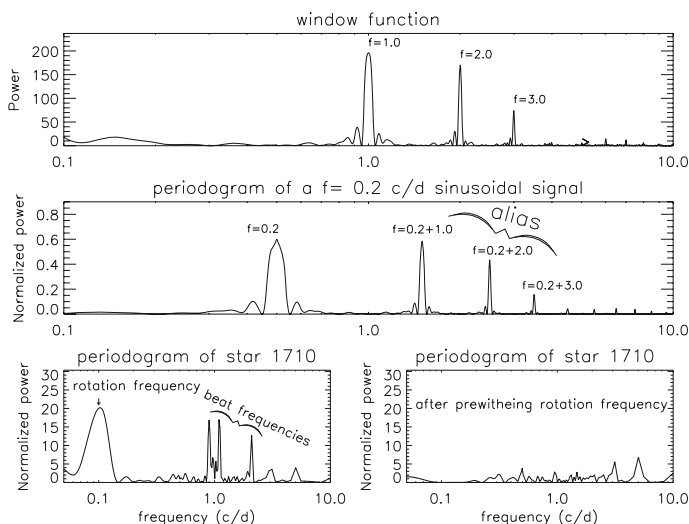


Fig. 3. *Top panel:* typical window function deriving from the data sampling and total time interval of the M11 observations. *Middle panel:* aliasing effect of the window function on an example periodic signal with frequency $f = 0.2 \text{ cd}^{-1}$. *Bottom left panel:* periodogram of star 1710 with rotation frequency, together with its beat frequencies. *Bottom right panel:* disappearance of beat frequencies after prewhitening the rotation frequency.

turn, is the probability that a peak of this height is simply caused by statistical variations, i.e. white noise. The normalized power corresponding to an $FAP = 0.01$ was found to be $P_N = 9.2$.

3.3. Alias detection

To identify the true periodicities in the periodogram, it is crucial to consider that a few peaks, even with high power, are aliases arising from both the data sampling and the total duration of the observation run. Inspection of the spectral window function helps identify which peaks in the periodogram may be aliases.

In the top panel of Fig. 3, we plot an example of the spectral window function of our data. Because of the sampling interval of about 1 day imposed by the rotation of the Earth and the fixed longitude of the observation site, the window function has major peaks at $f = \pm n \text{ cd}^{-1}$ (n integer), together with smaller sidelobes in the range $f = 1 \pm 0.1 \text{ cd}^{-1}$ around the major peak.

In the middle panel of Fig. 3, we plot the effects of the spectral window function on a strictly periodic signal of $f = 0.2 \text{ cd}^{-1}$ as an example with the same data sampling as the real data. Apart from the power peak corresponding to the true periodic signal at $f = 0.2 \text{ cd}^{-1}$, a number of alias peaks appear as a consequence of the convolution of the power spectrum and the window function. All these alias periods are beat periods (B) between the star’s rotation period (P) and the data sampling, and they obey the relation

$$\frac{1}{B} = \frac{1}{P} \pm n \quad (n = 1, 2, 3, \dots) \quad (1)$$

One method of checking whether peaks at short periods are beat periods is to perform a prewhitening of the data time series by fitting and removing a sinusoid with the star’s rotation period from the data.

In the bottom left panel of Fig. 3, we plot the case of star 1710 whose periodogram shows four peaks with a confidence level over 99%. Assuming that the highest peak at about $f = 0.09 \text{ cd}^{-1}$ indicates the star’s rotation frequency, we see in the bottom right panel of Fig. 3 that, after removing the primary

frequency from the data time series and recomputing the periodogram, all the other peaks actually disappear, confirming that they are actually beat frequencies.

3.4. Uncertainty with the rotation periods

To compute the error associated with the periods, we followed the method used by Lamm et al. (2004) where the uncertainty can be written as

$$\Delta P = \frac{\delta \nu P^2}{2}, \quad (2)$$

where $\delta \nu$ is the finite frequency resolution of the power spectrum and is equal to the full width at half maximum of the main peak of the window function $w(\nu)$. If the time sampling is fairly uniform, which is the case related to our observations, then $\delta \nu \approx 1/T$, where T is the total time span of the observations. From Eq. (2) it is clear that the uncertainty not only depends on the frequency resolution (total time span) but is also proportional to the square of the period. We also computed the error on the period following the prescription suggested by the Horne & Baliunas (1986), which is based on the formulation given by Kovacs (1981). The uncertainty computed according to Eq. (2) was found to be factor 5–10 larger than by the technique of Horne & Baliunas (1986). In this paper we report the error computed with Eq. (2). It thus can be considered as an upper limit, and the precision in the period could be better than what we quote in this paper.

4. Results

Our period search allowed us to detect 75 new periodic variables in the $22.2' \times 22.2'$ FoV centered on M11. The results are summarized in Table 1, where we list the following information: internal Identification Number (ID); Webda identification number; coordinates (J2000); periodicity (P) and its uncertainty (ΔP); normalized peak power (P_N); average V magnitude ($\langle V \rangle$); dereddened $(B - V)_0$ color; photometric accuracy (σ_{acc}); light curve amplitude (ΔV). The last was computed as the difference between the median values of the upper and lower 15% light curve normal points (see, e.g., Herbst et al. 2002). That prevents overestimating the amplitude due to possible residual outliers. We list a note about the membership probability to the cluster, as discussed in the next section: “a” is for high-probability members; “b” for lower-probability members; “n” for non-members. Finally, we indicate with a flag “y” the eclipsing binary systems as classified on the basis of the shape of their light curve. In Fig. 4 we plot, as an example, the results of period search for the stars 25 585 and 26 026. From the left to right panels we plot: (i) the V -band magnitude vs. time with overplotted the uncertainties; (ii) the phased light curve, which is folded by using the derived period; (iii) the Scargle periodogram. The complete set of 75 light curves, together with Scargle periodograms, are found in the online Figs. 10–25.

5. Discussion

Our major aim is to determine the rotation period distribution and the activity levels of the late-type members of M11. Therefore, we first have to identify the cluster members among the 75 newly discovered periodic variables, and subsequently to select only the late-type members whose discovered periodicity is likely related to stellar rotation. We exclude evident eclipsing

Table 1. Summary of period search.

ID	ID Webda	Right asc. (hh:mm:ss)	Declination (dd:mm:ss)	Period (d)	Norm. $\langle V \rangle$ Power (mag)	$(B - V)_0$ (mag)	σ_{acc} (mag)	ΔV (mag)	Memb. prob.	Binary
185	241	18:51:36.204	-06:16:40.24	0.94 ± 0.01	15.98	13.91	1.59	0.0094	0.0602	n
195	253	18:51:35.597	-06:09:11.90	0.466 ± 0.003	16.73	14.74	0.66	0.0111	0.0483	n
227	290	18:51:33.843	-06:20:27.27	0.94 ± 0.01	21.06	14.09	1.52	0.0073	0.1116	n
414	493	18:51:22.576	-06:21:51.37	0.249 ± 0.001	15.08	14.24	0.20	0.0793	0.1723	b
444	525	18:51:20.999	-06:14:01.33	0.249 ± 0.001	15.93	14.48	0.43	0.0096	0.0762	b
530	617	18:51:17.083	-06:13:39.61	0.95 ± 0.01	16.19	13.48	1.97	0.0093	0.0980	n
957	1075	18:51:04.289	-06:25:05.07	0.92 ± 0.01	27.22	13.09	1.64	0.0090	0.0817	n
1292	1433	18:50:55.568	-06:23:36.96	0.95 ± 0.01	16.26	11.63	-0.08	0.0080	0.0444	a
1509	1660	18:50:45.538	-06:12:54.69	2.19 ± 0.08	22.77	14.57	0.54	0.0114	0.0512	a
1606	1763	18:50:40.704	-06:14:44.25	1.23 ± 0.02	16.58	14.03	0.66	0.0076	0.0383	n
1647	1805	18:50:38.869	-06:13:12.26	0.94 ± 0.01	19.10	12.92	1.59	0.0074	0.0742	n
1663	1822	18:50:38.184	-06:13:51.35	1.18 ± 0.02	16.42	12.20	1.05	0.0091	0.0647	n
1719	1880	18:50:35.151	-06:12:50.15	5.4 ± 0.4	17.45	13.76	0.52	0.0103	0.0319	n
1733	1896	18:50:34.613	-06:25:05.34	20.0 ± 0.7	40.27	14.28	2.00	0.0112	0.1112	n
2098	...	18:51:00.154	-06:14:49.72	0.434 ± 0.009	28.45	12.37	0.00	0.0212	0.1073	b
3662	5005	18:50:28.031	-06:10:09.14	0.95 ± 0.01	23.17	14.20	1.74	0.0173	0.0596	n
3860	5203	18:50:32.581	-06:14:57.60	5.5 ± 0.4	22.06	14.80	1.74	0.0099	0.0729	n
3867	5210	18:50:32.763	-06:20:04.30	1.05 ± 0.01	32.74	13.95	1.98	0.0272	0.0918	n
3987	5330	18:50:35.453	-06:09:19.30	1.06 ± 0.01	22.89	15.23	1.72	0.0197	0.0911	n
4061	5404	18:50:37.144	-06:10:04.81	0.822 ± 0.003	16.67	15.25	0.58	0.0167	0.0465	a
4122	5465	18:50:38.537	-06:14:37.02	5.5 ± 0.4	18.98	14.69	0.75	0.0111	0.0437	n
4197	5540	18:50:40.578	-06:22:35.36	1.97 ± 0.05	38.20	15.24	0.68	0.0202	0.0935	a
4244	5587	18:50:41.695	-06:12:57.87	0.82 ± 0.01	25.61	14.51	0.39	0.0157	0.0443	a
4291	5634	18:50:42.840	-06:15:42.38	0.95 ± 0.01	23.54	15.00	1.22	0.0141	0.1600	n
4341	5684	18:50:43.663	-06:16:53.12	1.08 ± 0.01	24.64	15.03	0.65	0.0122	0.0902	b
4370	5713	18:50:44.146	-06:12:07.95	1.24 ± 0.02	19.69	15.31	0.33	0.0362	0.0916	a
4374	5717	18:50:44.235	-06:14:34.73	1.25 ± 0.02	21.36	15.21	0.45	0.0346	0.0743	a
4547	5890	18:50:47.746	-06:21:29.32	1.21 ± 0.02	15.13	15.31	1.16	0.0132	0.0572	n
4549	5892	18:50:47.769	-06:10:33.49	5.5 ± 0.4	24.59	14.63	0.60	0.0201	0.0371	a
4556	5899	18:50:47.853	-06:11:06.86	14 ± 3	48.12	15.03	1.35	0.0159	0.2109	n
5367	6710	18:51:03.950	-06:23:03.13	6.1 ± 0.5	17.73	14.41	1.70	0.0074	0.0652	n
5477	6820	18:51:06.144	-06:10:08.84	5.7 ± 0.5	27.66	14.83	1.50	0.0131	0.1068	n
6370	7713	18:51:22.449	-06:11:15.40	5.7 ± 0.5	25.76	15.30	0.76	0.0173	0.0650	b
6428	7771	18:51:23.829	-06:25:36.70	4.0 ± 0.2	30.36	14.73	0.59	0.0099	0.0710	a
6440	7783	18:51:24.012	-06:13:20.38	1.888 ± 0.003	39.03	14.50	1.38	0.0090	0.0816	n
6756	8099	18:51:31.434	-06:13:53.09	5.8 ± 0.5	17.80	14.94	1.84	0.0154	0.0968	n
8594	10 095	18:51:10.248	-06:06:01.43	1.244 ± 0.005	15.68	17.14	0.39	0.0609	0.1338	n
9517	10 696	18:51:41.247	-06:07:18.46	0.88 ± 0.01	20.16	15.32	1.20	0.0129	0.1028	n
10 052	11 078	18:51:19.119	-06:07:55.82	7.4 ± 0.8	15.01	15.72	0.85	0.0197	0.0591	n
10 161	11 155	18:50:41.777	-06:08:03.78	21.05 ± 0.01	41.28	16.54	1.24	0.0552	0.3606	n
10 851	11 629	18:50:55.996	-06:09:02.21	4.6 ± 0.3	17.85	15.56	0.68	0.0146	0.0500	b
10 861	11 637	18:50:54.708	-06:09:02.51	5.2 ± 0.4	16.05	16.68	0.61	0.0568	0.1264	b
12 485	12 774	18:50:54.307	-06:11:09.85	5.2 ± 0.4	30.33	15.79	0.60	0.0150	0.0691	b
12 646	12 890	18:50:52.443	-06:11:23.12	2.6 ± 0.1	23.89	15.74	0.55	0.0150	0.0575	b
13 073	13 214	18:51:12.981	-06:11:58.35	1.22 ± 0.02	15.74	15.78	1.46	0.0202	0.0809	n
13 511	13 536	18:51:44.895	-06:12:34.27	0.327 ± 0.001	33.78	16.28	0.46	0.0419	0.2369	b
13 540	13 556	18:50:56.759	-06:12:35.98	5.3 ± 0.4	15.95	15.57	0.81	0.0237	0.0752	n
13 951	13 849	18:51:37.563	-06:13:11.24	1.25 ± 0.02	18.47	16.95	0.79	0.0718	0.1666	b
14 095	13 950	18:50:48.687	-06:13:24.10	3.5 ± 0.1	18.25	16.18	0.57	0.0339	0.1054	b
14 450	14 207	18:50:27.796	-06:13:55.76	2.5 ± 0.1	24.80	16.53	0.90	0.0467	0.1442	b
15 291	14 792	18:51:18.248	-06:15:18.63	0.83 ± 0.01	15.54	16.05	1.13	0.0312	0.0781	n
15 633	15 020	18:50:43.468	-06:15:50.88	5.6 ± 0.4	18.04	15.66	1.58	0.0172	0.0428	n
17 415	16 297	18:51:26.378	-06:18:44.88	0.420 ± 0.002	18.54	16.03	0.59	0.0217	0.0801	b
17 546	16 397	18:50:39.657	-06:18:53.31	0.83 ± 0.01	16.12	17.00	1.10	0.0989	0.3246	n
17 649	16 470	18:50:30.580	-06:19:03.98	0.362 ± 0.002	22.86	16.89	0.94	0.2341	0.3098	b
17 730	16 528	18:50:41.216	-06:19:05.59	5.2 ± 0.4	22.95	16.67	1.12	0.0311	0.1987	n
18 776	17 281	18:51:10.130	-06:20:29.10	4.8 ± 0.3	18.16	16.52	0.61	0.0364	0.1463	b
19 357	17 726	18:50:35.405	-06:21:13.05	1.18 ± 0.02	17.35	16.25	0.69	0.0259	0.1019	b
19 570	17 883	18:50:51.008	-06:21:31.20	0.83 ± 0.01	22.48	15.87	0.52	0.0269	0.0753	b
19 844	18 088	18:50:41.003	-06:21:53.06	0.2214 ± 0.0007	40.20	15.98	1.16	0.0267	0.6817	n
21 243	19 140	18:50:39.625	-06:23:35.99	0.488 ± 0.003	15.20	16.15	0.70	0.1086	0.3077	b
22 541	20 108	18:50:53.732	-06:25:09.70	4.8 ± 0.3	19.88	16.50	0.78	0.0346	0.1428	b
23 809	21 055	18:51:17.696	-06:26:45.79	0.95 ± 0.01	27.95	17.06	0.96	0.0380	0.1921	b
23 878	21 104	18:50:36.522	-06:26:49.94	1.85 ± 0.01	23.06	16.68	1.00	0.0495	0.3521	n

Table 1. continued.

ID	ID	Right asc.	Declination	Period	Norm. $\langle V \rangle$	$(B - V)_0$	σ_{acc}	ΔV	Memb.	Binary	
	Webda	(hh:mm:ss)	(dd:mm:ss)	(d)	Power (mag)	(mag)	(mag)	(mag)	prob.		
25 585	22 164	18:50:30.755	-06:19:07.60	5.4 ± 0.4	25.54	17.32	1.37	0.0697	0.2707	n	
26 026	22 451	18:50:33.299	-06:24:22.86	0.81 ± 0.01	23.91	16.91	0.66	0.0561	0.1622	b	
26 072	22 483	18:50:29.833	-06:24:46.87	0.720 ± 0.009	16.18	18.13	0.94	0.1793	0.3507	b	
26 158	22 536	18:50:34.161	-06:25:35.99	3.2884 ± 0.04	25.61	16.52	0.62	0.0839	0.4506	b	y
27 360	23 360	18:51:01.356	-06:11:07.67	0.396 ± 0.002	23.60	15.76	0.39	0.0296	0.1788	b	
29 011	24 388	18:51:45.297	-06:21:07.52	2.38 ± 0.09	16.53	16.36	0.74	0.0744	0.1153	b	y
29 195	...	18:50:27.943	-06:05:40.81	0.95 ± 0.01	20.24	17.12	0.00	0.0918	0.2132	n	y
30 166	25 180	18:51:01.500	-06:18:41.95	1.23 ± 0.02	20.62	15.47	0.40	0.0243	0.0715	b	
30 525	25503	18:51:29.387	-06:15:22.32	0.639 ± 0.006	32.82	16.41	0.82	0.0357	0.1778	b	
34 773	26 477	18:50:22.444	-06:13:50.70	1.23 ± 0.4	18.01	16.20	0.72	0.0279	0.0886	b	
35 526	26763	18:50:56.030	-06:09:42.59	5.0 ± 0.3	27.36	16.73	1.14	0.0435	0.2130	n	

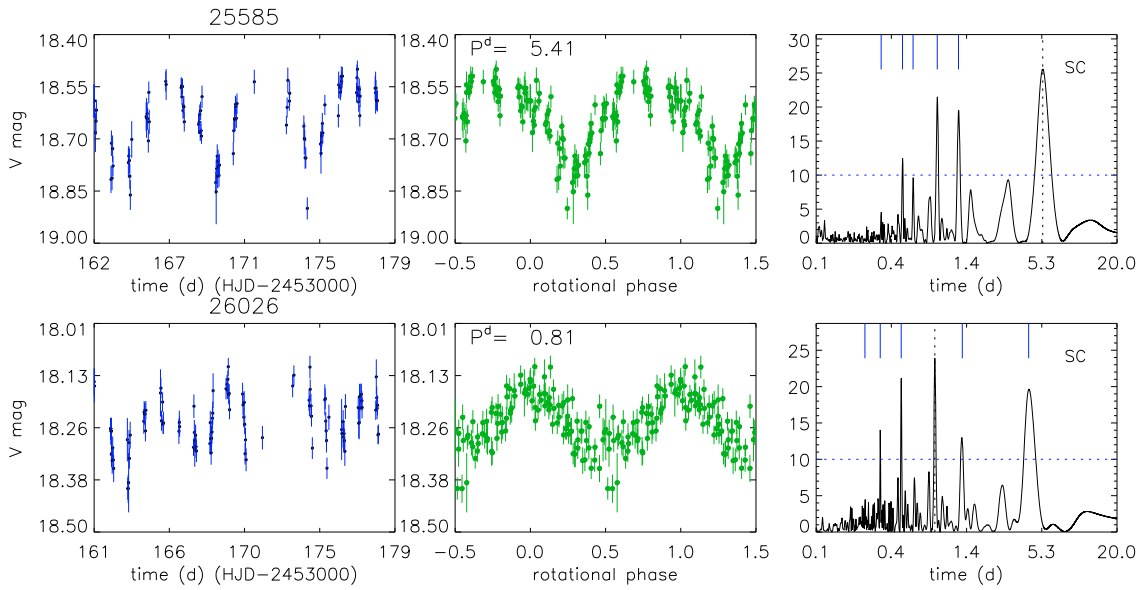


Fig. 4. From left to right: V -band data time series with uncertainties; folded light curves with phases computed by using the derived period; Scargle normalized periodogram. The vertical dashed line indicates the major peak related to the rotation period, whereas the solid top bars indicate its beat periods. The horizontal dotted line indicates the 99% confidence level.

binaries from the final sample of periodic late-type members. In fact, the tidal synchronization of the components of close binary systems means that their rotational evolution significantly differs from the evolution history of single stars, on which we are focused.

5.1. Candidate member selection

M11 has a very rich stellar background, and it is a very difficult task to identify the cluster members. The proper motion studies carried out by McNamara et al. (1977), Su et al. (1998), and Dias et al. (2006) only provide information on the bright ($V < 16$ mag) members. The radial velocity survey carried out by Mathieu et al. (1986) is also limited to a handful of stars. Our proposed periodic variables have information neither on proper motion nor on radial velocity, so we use the following two criteria to identify cluster members: i) the photometric membership, which is the distance of any star from the theoretical isochrone in the color-magnitude diagram (see, e.g., Irwin 2006, 2008); ii) the spatial distance from the cluster center.

In Fig. 5 we plot the color-magnitude V vs. $B - V$ (left panel) and V vs. $V - I$ (right panel) diagrams of all stars detected in our FoV. The $B - V$ colors are ours, whereas the $V - I$ colors

are taken from Sung et al. (1999) and available only for stars brighter than $V \approx 16.7$. We overplot the color-reddened 230-Myr isochrone derived from Girardi et al. (2000) and corresponding to the cluster parameters taken from Sung et al. (1999).

In the first criterion, we assign two probability levels on the basis of the distance from the isochrone: “1a” and “1b” to stars with distance respectively smaller (blue small dots in Fig. 5) or larger (black small dots) than $\pm(1.4 + \sigma)$ mag in the case of V vs. $B - V$ diagram. Similarly, we assign “2a” and “2b” in the case of the V vs. $V - I$ diagram. The quantity σ takes the increasing photometric uncertainty towards fainter stars into account.

In the second criterion, we assign two probability levels on the basis of the projected angular distance from the cluster center and the relative density distribution shown in Fig. 6: “3a” to stars with distance less than $10'$, “3b” to stars with distance over $10'$.

As a final result, we assign a high-probability flag “a” to stars simultaneously having “1a”, “2a”, and “3a”; a lower-probability flag “b” to stars having “1a”, “3a” and no measured $V - I$ color. All the remaining stars are classified as non members “n” so are excluded from the analysis of the cluster rotation period distribution. The probability flags are listed in Table 1.

Our final sample of newly discovered variables consists of 9 high-probability members (4 early-type stars with $(B - V)_0 < 0.5$,

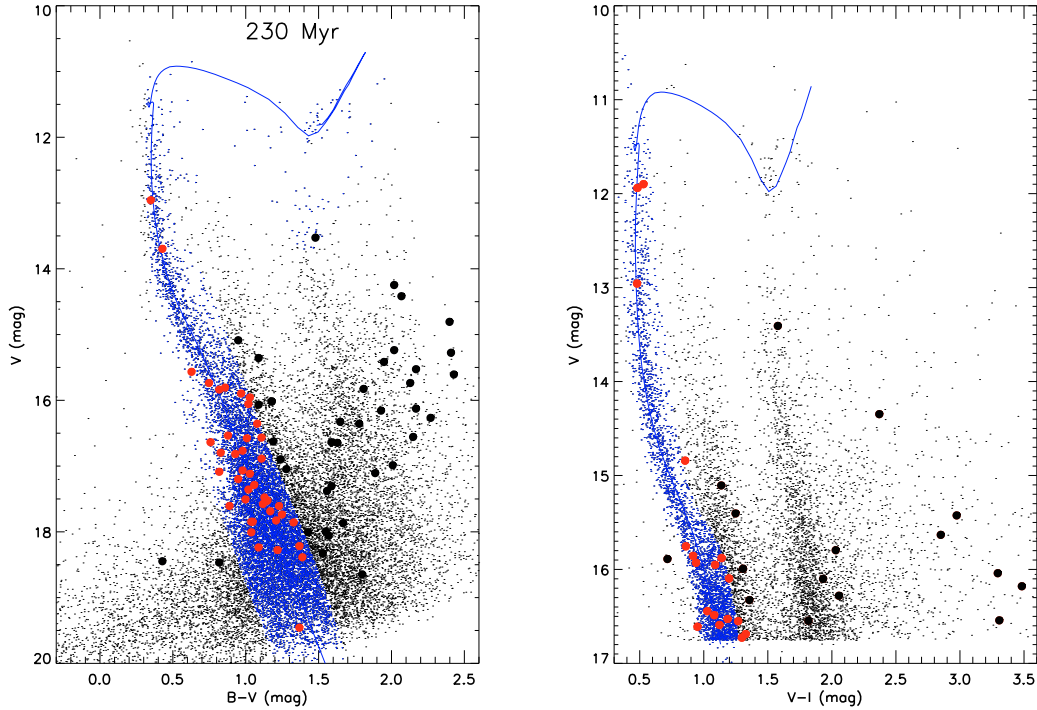


Fig. 5. *Left panel:* V vs. $B - V$ diagram of the stars (dots) detected in the $22.2' \times 22.2'$ field of M 11. Photometric candidate members are plotted with small blue bullets, newly-discovered periodic stars are plotted with large red (high and low probability members) and black bullets (non members). The solid line represents the isochrone corresponding to an age of $\log t = 8.35$, $E(B - V) = 0.428$ mag, $(m - M) = 12.69$ mag (Sung et al. 1999). *Right panel:* same as left panel but with $V - I$ colors from Sung et al. (1999). Neither V nor $V - I$ values are available for stars fainter than ~ 16.7 .

5 late-type stars with $(B - V)_0 \geq 0.5$), 29 lower-probability members (2 early-type, 25 late-type, 2 eclipsing binaries), 37 non members not considered in the following analysis. In Fig. 7 we plot the 2 newly discovered eclipsing binary cluster members.

5.2. Rotation period distribution

As anticipated, our attention is focused on the late-type members of M 11. In fact, the detected periodicity of these late-type stars most likely represents the stellar rotation period. The variability observed over time scales from several hours to days arises from non-uniformly distributed, cool-spotted regions on the stellar photosphere, which are carried in and out of view by the star’s rotation. We excluded from our analysis all periodic variables bluer than $(B - V)_0 = 0.5$, whose periodic variability is likely related to pulsations. We also excluded the already known (see Koo et al. 2007), as well as the newly discovered W UMa-type and detached eclipsing binaries, because their angular momentum evolution is altered by tidal synchronization between stellar components.

All periodic members discovered by us have $(B - V)_0 < 0.9$, which roughly corresponds to main sequence stars of spectral type earlier than K2/3 and mass $M/M_\odot \gtrsim 0.8$. Therefore, our analysis has provided the first rotation period distribution of the G-type and early-K members of M 11. The absence of periodic middle-K or later-type stars must be ascribed to the lower photometric accuracy, which becomes comparable to or larger than the periodic variability amplitude due to starspots for the fainter stars.

In Fig. 8 we plot the rotation period distribution of late-type (bona-fide) single stars vs. the $(B - V)_0$ color. Different symbols are used to plot stars with different levels of membership probability to the cluster, according to the criteria outlined in the

previous section. Specifically, 5 stars are high-probability members (filled bullets) and 16 stars are low-probability members (open circles). Here we recall that such a lower probability level of membership arises from the unavailability of $V - I$ measurements (see right panel of Fig. 5). In the following analysis, we consider both stars with “a” and “b” membership probability all together, although plotted with different symbols.

A slightly younger cluster (about 200 Myr) with known rotational properties is M 34 (Irwin et al. 2006). The survey of Irwin et al. (2006) allows the rotation period distribution of the lower-mass K-M stars to be determined. In Fig. 8 we plot the 16 periodic variables of M 34 with spectral type earlier than K2. The original $(V - I)_0$ colors in Irwin et al. have been transformed into $(B - V)_0$ colors by using standard stars color-color relations (Cox 2000). These additional data allow us to get a more numerous sample of periodic stars and, consequently, to derive a reliable rotation period distribution of G0-K2 stars at an age of about 200–230 Myr.

As observed in other young open clusters, the M 11 members are also found to be distributed between two different rotation regimes. There is a fraction of stars whose rotation period is longer than about 1–2 days. Their distribution displays an upper envelope that increases with increasing $B - V$ color. These stars belong to the so-called “interface sequence”, according to the classification scheme of Barnes (Barnes 2003). These stars have experienced the effects of rotation braking by stellar magnetized winds, and are expected to continue slowing down to reach, by an age of about 500–600 Myr, a one-to-one dependence between rotation period and color (see, e.g., Collier Cameron et al. 2009). A second fraction of stars with period shorter than 1–2 days belongs to the so-called “convective sequence”. They have not yet experienced significant spin down and are progressively moving towards the interface sequence of slow rotators. Bluer stars

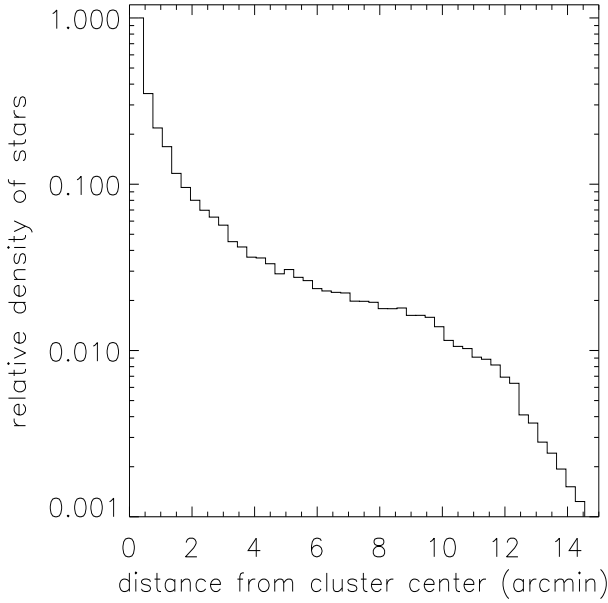


Fig. 6. Relative density of stars in the M11 FoV with respect to the cluster center.

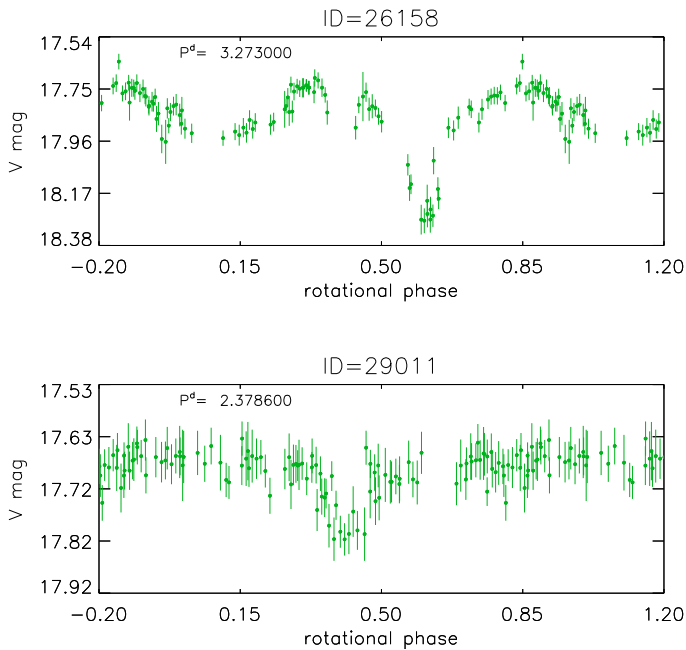


Fig. 7. Eclipsing binaries newly discovered among periodic members of M11.

in this sequence leave first, and the $B - V$ color at which the sequence begins varies with the cluster age. The solid line in Fig. 8 represents the theoretical curve, computed by using Eq. (1) of Barnes (2003)

$$P = \sqrt{t} f(B - V) \quad (3)$$

where $f(B - V)$ represents the color dependence of the rotation period. It represents the expected upper envelope of the rotation period distribution at a nominal age of ~ 230 Myr, assuming a rotational rate decay according to the Skumanich law (Skumanich 1972). We refer the reader to Barnes (2003) for a detailed description of both sequences. The agreement between the observed interface sequence, and its expected distribution is quite good and supports the estimated cluster age.

From our analysis we find that the G-type members of M11 have a median rotation period of $P = 4.8$ days. This is the first determination of median rotation period of G-type stars at an age of 230 Myr, which is the only available value in the age range from 150 Myr (M35) to 550 Myr (M37).

5.3. Angular momentum evolution

The variation in time of the median rotation period of cluster members is the quantity generally used to detect and investigate the rotational evolution of low-mass stars.

In the right panel of Fig. 8, we compare the rotation period distribution of M11 with the distributions of the younger open cluster M35 (150 Myr; Meibom et al. 2009) and of the older open cluster M37 (550 Myr; Hartman et al. 2009; Messina et al. 2008). Focusing our attention on the G-type slowly rotating stars of these clusters, that is, on stars in the interface sequence and in the $0.55 < (B - V)_0 < 0.9$ color range, we find that the median rotation periods are $P_{M35} = 4.4$ d, $P_{M11} = 4.8$ d, and $P_{M37} = 6.8$ d. This is the major result of our analysis: we have determined the median rotation period of G stars at an age of 230 Myr, at which no information on rotational properties has been available to date. Moreover, the comparison with the median period of two other clusters shows that the value we found is consistent with the expected rotation slow down with age. We plot the age-parameterized family of theoretical curves corresponding to nominal ages of ~ 150 Myr, ~ 230 Myr, and ~ 550 Myr. The younger gyro-isochrones (150 and 230 Myr) appear to fit the observed distribution upper envelopes better than the older gyro-isochrone at 550 Myr. However, this discrepancy depends on the parametric curve rather than on the age of M37, which is quite well established (see Hartman et al. 2009). Two important results arise from comparing data with isochrones. First, the agreements show the validity of the Skumanich rotation rate decay, which is a dependence of rotation on square root of time. Second, the Barnes parameterization reproduces the observed rotation period distribution very well at an age of about 230 Myr.

Now we turn our analysis to the fast rotators. In this case we note some sort of discrepancy with respect to the younger cluster M35. In fact, in M35 the convective sequence begins approximately at $(B - V)_0 = 0.8$. We expect such a sequence to begin at redder colors in older clusters. On the contrary, we note a number of fast rotating stars bluer than $(B - V)_0 < 0.8$ in both M34 and M11. Actually, this discrepancy may be explained without need of contradicting the rotation evolutionary sequence described above. First, we see that these unexpected blue fast rotators have a lower membership probability. As discussed by Sung et al. (1999), the cluster is at low galactic latitude ($\sim -3^\circ$), near the Scutum star cloud and the Sagittarius-Carina arm, resulting in very large contamination of the cluster color-magnitude diagram from the relatively young (and, therefore, rapidly rotating) field population. Therefore, these blue fast rotators may well be interlopers. Alternatively, some of these fast rotators may be cluster members, but they may belong to close binaries of BY Dra, RS CVn, W UMa or FK Com types, which have not yet been identified as such a kind of variables, and are rapidly rotating due to tidal interaction and synchronization. Indeed, all the already known and newly discovered binary stars with $(B - V)_0 > 0.5$ and with high-probability membership, if plotted in Fig. 8, would all populate the convective sequence. A third possibility may be false detections of the periods. For example, the presence of two activity centers in the stellar photosphere at the epochs of observations, about 180° away in longitude from each other, can produce a light modulation with half

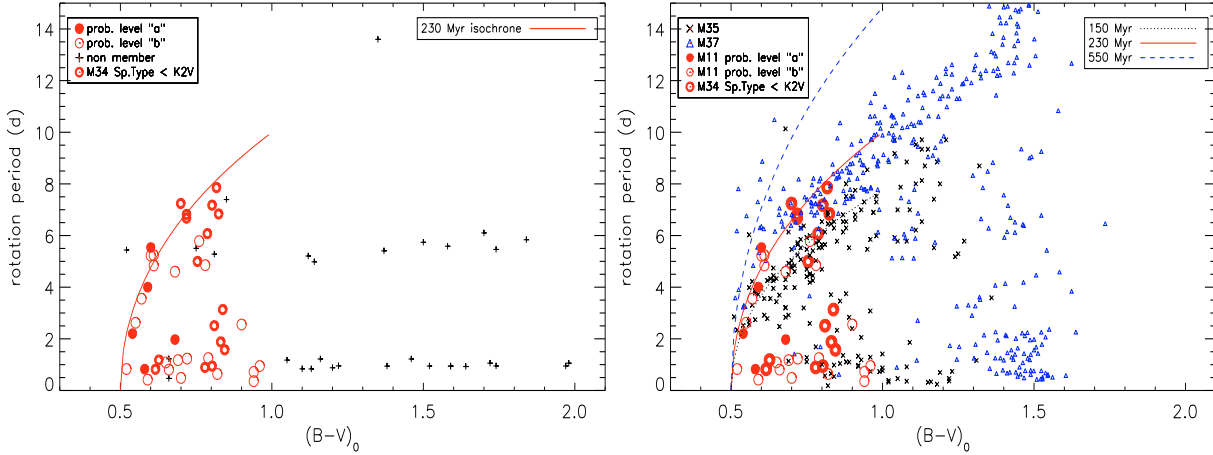


Fig. 8. *Left panel:* rotation period vs. $(B - V)_0$ colour for the members of M11. Different symbols are used to represent high- and low membership probability. The periods of the M34 members with spectral type earlier than K2/3 are also plotted. The solid curve represents the gyro-isochrone at a nominal age of 230 Myr. *Right panel:* same as left panel, but with overplotted the rotation period distribution of M37 (triangles) and M35 (asterisks). The family of age-parameterized curves from gyrochronology corresponding to ages of 150, 230 and 550 Myr is overplotted.

of the true rotation period. In these cases, consecutive observation seasons are needed to detect the true rotation period (Parihar et al. 2009).

5.4. Photospheric activity

The photometric variability we observed in the proposed late-type periodic members of M 11 arises from cool photospheric spots whose visibility is modulated by the stellar rotation. The total amount of cool spots is related to surface magnetic fields, whose filling factor depends on the rotation rate and on the depth of the convection zone (or mass). The amplitude of the observed variability, specifically the peak-to-peak light curve amplitude, is suitable for tracing the dependence of the magnetic-field filling factor on rotation and mass. In Fig. 9 we plot the amplitude of the V -band light curve of the M 11 late-type periodic members, together with the M34 members. The symbols have same meaning as in Fig. 8. We see that the upper envelope of the light curve amplitude decreases with increasing rotation period. This is consistent with the expected dependence on rotation rate of the efficiency of magnetic field generation and intensification by an $\alpha\Omega$ dynamo. The solid line represents the fit to the upper envelope of the light curve amplitude distribution of slowly rotating Pleiades G stars (110 Myr) taken from Messina et al. (2001, 2003). With the data at our disposal, we do not see any significant difference between the 110-Myr and the 230-Myr distribution upper envelopes. Our sample of only G stars does not allow us to say anything about the mass dependence of the amplitude-rotation relation. As discussed in Paper I, there is some marginal (yet) evidence of some other age-dependent quantity, in addition to mass and rotation, that controls the level of (photospheric at least) activity and makes older stars less active than younger stars (see also Messina et al. 2010). A similar suspect has already been raised by Messina et al. (2001), who found evidence that, for a fixed mass and rotation period, the level of starspot activity increases (or alternatively the gross surface distribution of spots changes) from the zero-age main sequence up to the Pleiades age (~ 120 Myr) and then it decreases with age. With the data of M 11 G stars in hand, we can state that up to the M 11 age the level of activity remains at highest levels. On the contrary, the K-type stars at an age of 200 Myr already show a significantly decreased activity with respect to the younger K-type Pleiades stars, as shown in Fig. 16 of Irwin et al. (2006).

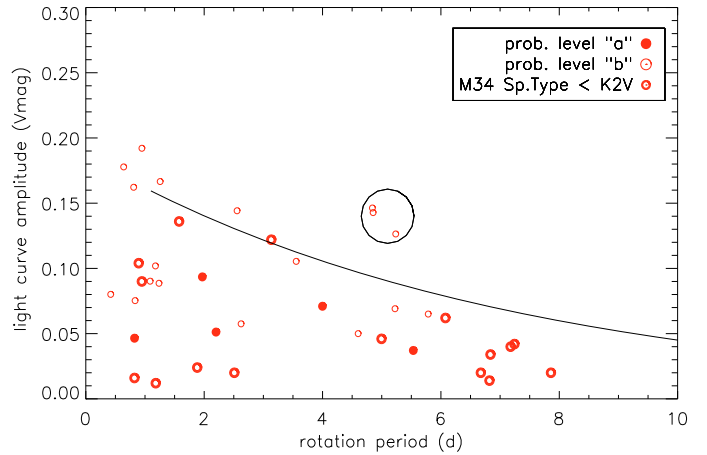


Fig. 9. V -band light curve amplitude (ΔV) vs. rotation period for the same stars plotted in the left panel of Fig. 8. The solid line represents the upper envelope of the ΔV vs. rotation period distribution of dwarf G stars from Messina et al. (2003), whereas the three circled stars above there are suspected binary stars.

It is interesting to note that, when we select the final sample of periodic variables to determine the rotation period distribution, the existence of a rotation-activity relation provides an independent tool for identifying either possible binary systems or erroneous period determination. In fact, because of eclipse minima and enhanced rotation with respect to single stars, close binaries show light curve amplitudes that are much larger than observed in single stars. Similarly, an incorrect period determination, specifically an incorrect value higher than the true rotation period (e.g. its beat period), produces an outlier in the rotation-activity distribution. Such outliers allow us to identify, or at least to defer for additional study, stars that may contaminate the final sample. In our case, the stars 10 861, 18 776 and 22 541 (which are circled in Fig. 9) show a light curve amplitude larger than ever observed in stars of similar mass and rotation period. Follow-up observations may reveal that the adopted period is actually the (long) beat period. Similarly, this method can allow us to identify, and consequently exclude from the final sample, W-UMa close binaries whose light-curve amplitudes clearly

deviate from the distribution upper envelope and whose phased light-curve shapes are much scattered to identify its W UMa nature.

6. Conclusions

We have analyzed *V*-band magnitude time series of the young 230-Myr open cluster M 11 collected in 2004 at the LOAO observatory. Our analysis allowed us to derive the following results:

- We discovered 75 new periodic variables in a $22.2' \times 22.2'$ FoV centered on M 11. Considering that 64 periodic variables were known from earlier studies, the total number of known periodic variable in this FoV is 139.
- Two newly discovered periodic variable members are likely eclipsing binary systems. The discovery of such systems whose absolute physical parameters can be determined with spectroscopic and multiband photometric follow-up studies is relevant for better determining the distance to the cluster, as well as for understanding the dynamical evolution of binary systems at an intermediate age.
- Out of 75 new periodic variables, we found that 30 stars are probably single late-type periodic cluster members. Such stars have colors in the range $0.5 < (B - V)_0 < 0.9$, which corresponds to a main sequence spectral type earlier than K2 and stellar mass higher than $0.8 M_{\odot}$.
- By adding to our data 16 G-type periodic variables belonging to the almost coeval cluster M 34 and taken from the literature, we determined the median rotation period $P = 4.8$ d of the G stars at an age of about 200–230 Myr from a sample of 46 stars for the first time. In fact, the rotational properties of G stars in the age range 150–550 Myr were unknown before the present study.
- The median period we determined is longer than the median period $P = 4.4$ d of G stars in the younger cluster M 35 and shorter than the median period $P = 6.8$ d of G stars in the older cluster M 37. This result is in good agreement with the expected scenario of rotation spin down with age according to the Skumanich rotation decay law.
- The distribution of the light curve amplitude of G-type members of M 11 is found to decrease with increasing rotation period. This activity-rotation relation is found either in other open clusters or in field stars, and it supports the expected operation of an $\alpha\Omega$ dynamo whose efficiency is related to both rotation and convection zone depth. The average level of activity of these 230 Myr old stars is found to be comparable to the activity level of the younger Pleiades stars.

Acknowledgements. This work was supported by the Italian Ministero dell'Università, Istruzione e Ricerca (MIUR) and the National Institute for Astrophysics (INAF). The extensive use of the SIMBAD and ADS databases operated by the CDS, Strasbourg, France, is gratefully acknowledged. This research made use of the WEBDA database, operated at the Institute for Astronomy of the University of Vienna. S.-C.R. acknowledges support from National

Research Foundation of Korea (NRF) grant funded by the Korea government (MEST) (N. 2009-0062863). We thank the referee for very useful comments and suggestions.

References

- Bailer-Jones, C. A. L., & Mundt, R. 2001, A&A, 367, 218
 Barnes, S. 2003, ApJ, 586, 464
 Barnes, S. 2007, ApJ, 669, 1167
 Bouvier, J., Forestini, M., & Allain, S. 1997, A&A, 326, 1023
 Cox, A. N. 2000, in *Allen's Astrophysical Quantities*, 4th edn (Springer, AIP Press)
 Girardi, L., Bressan, A., Bertelli, G., et al. 2000, A&AS, 141, 371
 Gonzalez, G., & Wallerstein, G. 2000, PASP, 112, 1081
 Guinan, E. F., McCook, G. P., DeWarf, L. E., et al. 2003, BAAS, 35, 766
 Dias, W. S., Assafin, M., Flório, V., Alessi, B. S., & Líbero, V. 2006, A&A, 446, 949
 Hargis, J. R., Sandquist, E. L., & Bradstreet, D. H. 2005, AJ, 130, 2824
 Hartman, J. D., Gaudi, B. S., Pinsonneault, M. H., et al. 2009, ApJ, 691, 342
 Herbst, W., & Wittenmyer, R. 1996, BAAS, 28, 1338
 Herbst, W., Bailer-Jones, C. A. L., Mundt, R., Meisenheimer, K., & Wackermann, R. 2002, A&A, 396, 513
 Herbst, W., & Mundt, R. 2005, ApJ, 633, 967
 Hodgkin, S. T., Irwin, J. M., Aigrain, S., et al. 2006, AN, 327, 9
 Holzwarth, V., & Jardine, M. 2007, A&A, 463, 11
 Horne, J. H., & Baliunas, S. L. 1986, ApJ, 302, 757
 Irwin, J., Aigrain, S., Hodgkin, S., et al. 2006, MNRAS, 370, 954
 Irwin, J., Hodgkin, S., Aigrain, S., et al. 2007, MNRAS, 377, 741
 Irwin, J., Hodgkin, S., Aigrain, S., et al. 2008, MNRAS, 383, 1588
 Ivanova, N., & Taam, R. E. 2003, ApJ, 599, 516
 Kang, Y. B., Kim, S.-L., Rey, S.-C., et al. 2007, PASP, 119, 239
 Kawaler, S. D. 1988, ApJ, 333, 236
 Kim, S.-L., Chun, M.-Y., Park, B.-G., et al. 2001, A&A, 371, 571
 Koo, J.-R., Kim, S.-L., Rey, S.-C., et al. 2007, PASP, 119, 1233
 Kovacs, G. 1981, Ap&SS, 78, 175
 Krishnamurthi, A., Pinsonneault, M. H., Barnes, S., et al. 1997, ApJ, 480, 303
 Lamm M. H., Bailer-Jones, C. A. L., Mundt, R., Herbst, W., Scholz, A. 2004, A&A, 417, 557
 MacGregor, K. B., & Brenner, M. 1991, ApJ, 376, 204
 Martín, E. L., Dahm, S., & Pavlenko, Y. 2001, ASP Conf. Ser. 245, ed. T. von Hippel, C. Simpson, & N. Manset (San Francisco), 349
 Mathieu, R. D., & Latham, D. W. 1986, AJ, 92, 1364
 McNamara, B. J., Pratt, N. M., & Sanders, W. L. 1977, A&AS, 27, 117
 Meibom, S., Mathieu, R. D., & Stassun, K. G. 2009, ApJ, 695, 679
 Messina, S. 2007, Mem. Soc. Astron. It., 78, 628
 Messina, S., Rodonò, M., & Guinan, E. F. 2001, A&A, 366, 215
 Messina, S., Pizzolato, N., Guinan, E. F., et al. 2003, A&A, 410, 671
 Messina, S., Distefano, E., Parihar, P., et al. 2008, A&A, 483, 253
 Messina, S., Desidera, S., Turatto, M., Lanzafame, A. C., & Guinan, E. F. 2010, A&A, accepted
 Meynet, G., Mermilliod, J.-C., & Maeder, A. 1993, A&AS, 98, 477
 Parihar, P., Messina, S., Distefano, E., Shantikumar, N. S., & Medhi, B. J. 2009, MNRAS, 400, 603
 Press, W. H., Teukolsky, S. A., Vetterling, W. T., et al. 1992, in *Numerical recipes in FORTRAN* (Cambridge: University Press), 2nd edn
 Radick, R. R., Lockwood, G. W., Skiff, B. A., et al. 1995, ApJ, 452, 332
 Rebull, L. M., Wolff, S. C., & Strom, S. E. 2004, AJ, 127, 1029
 Roberts, D. H., Lehar, J., & Dreher, J. W. 1987, AJ, 93, 978
 Roze, M. B., & Hintz, E. G. 2007, AJ, 134, 2067
 Scargle, J. D. 1982, ApJ, 263, 835
 Sills, A., Pinsonneault, M. H., & Terndrup, D. M. 2000, ApJ, 534, 335
 Skumanich, A. 1972, ApJ, 171, 565
 Stassun, K. G., Mathieu, R. D., Mazeh, T., et al. 1999, AJ, 117, 2941
 Su, C.-G., Zhao, J.-L., & Tian, K.-P. 1998, A&AS, 128, 255
 Sung, H., Bessel, M. S., Lee, H.-W., Kang, Y.-H., & Lee, S.-W. 1999, MNRAS, 310, 982
 von Braun, K., Lee, B. L., Seager, S., et al. 2005, PASP, 117, 141

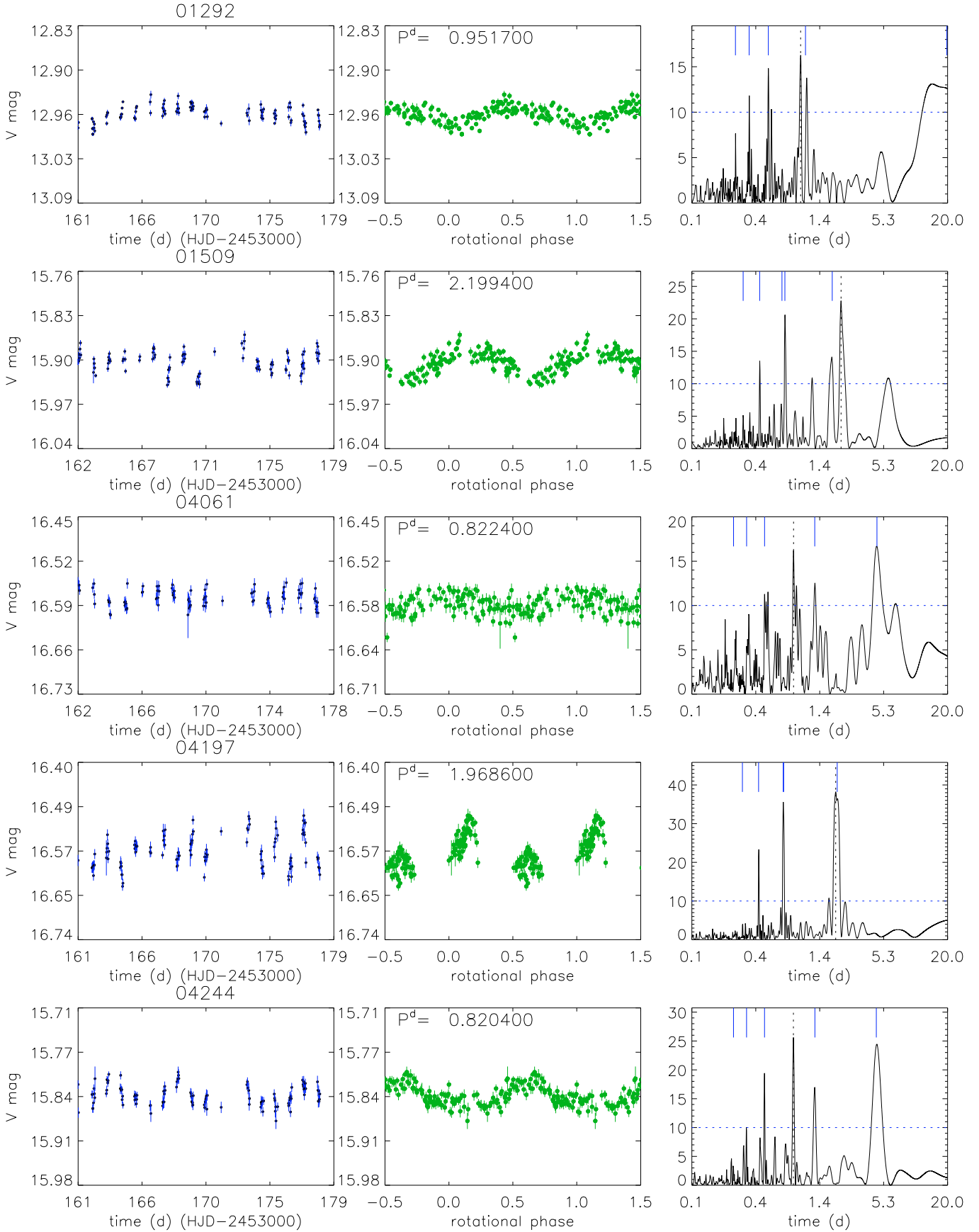


Fig. 10. High-probability “a” periodic candidate cluster members. *From left panel:* V-band time series, phased light curve, and Scargle periodogram. See Sect. 4 for a detailed description.

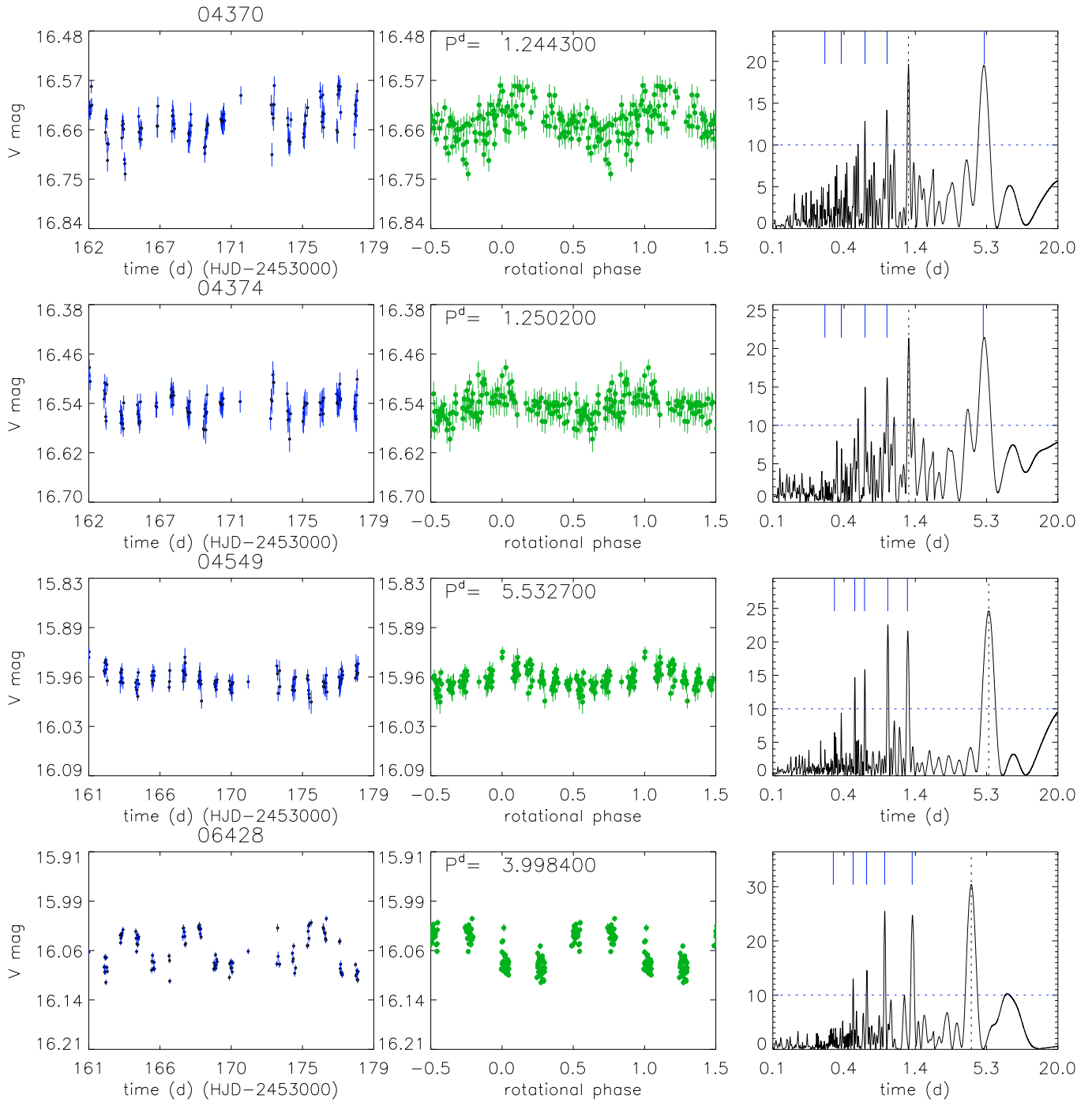


Fig. 11. As in Fig. 10.

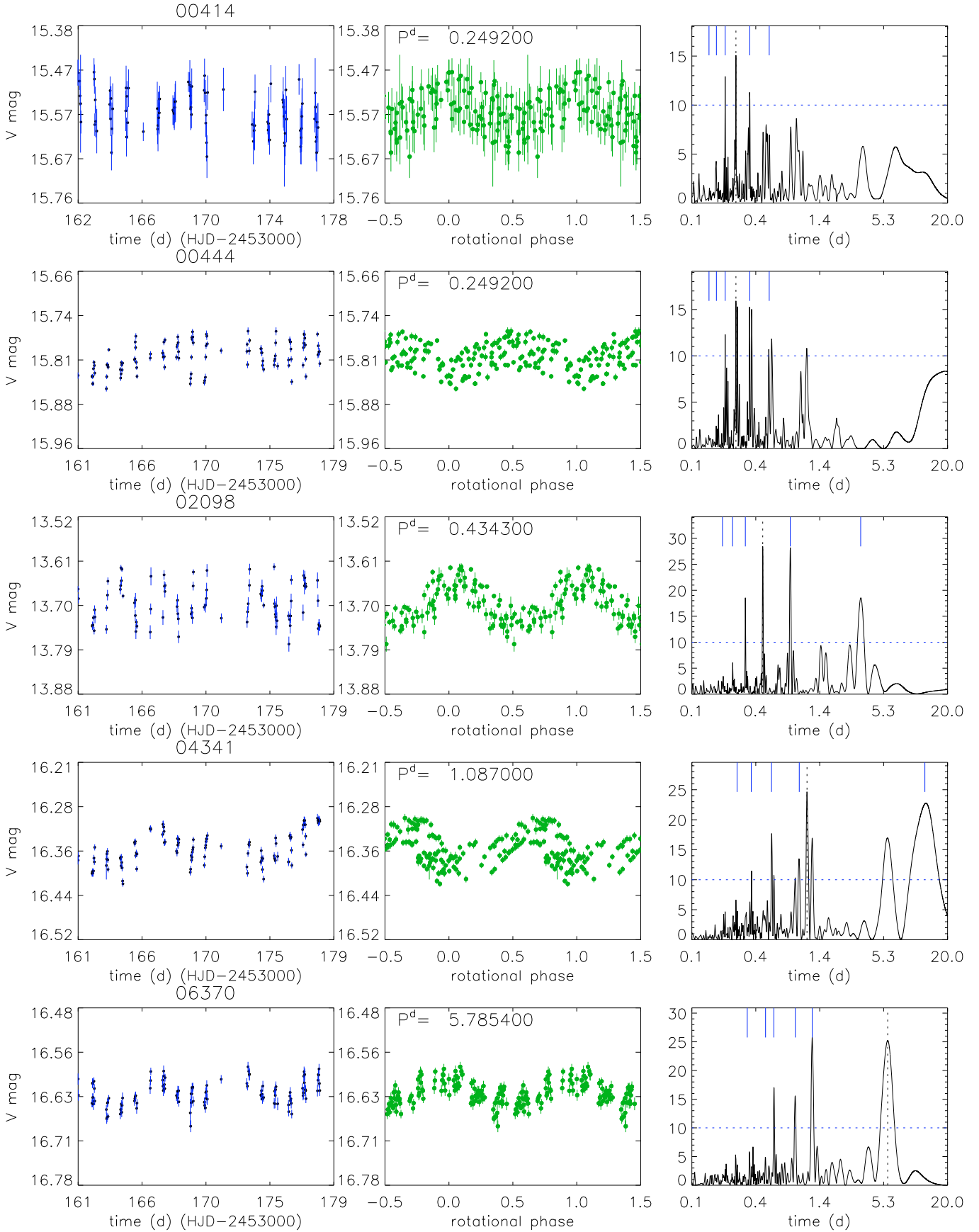


Fig. 12. Lower-probability “b” periodic candidate cluster members. *From left panel:* V-band time series, phased light curve, and Scargle periodogram. See Sect. 4 for a detailed description.

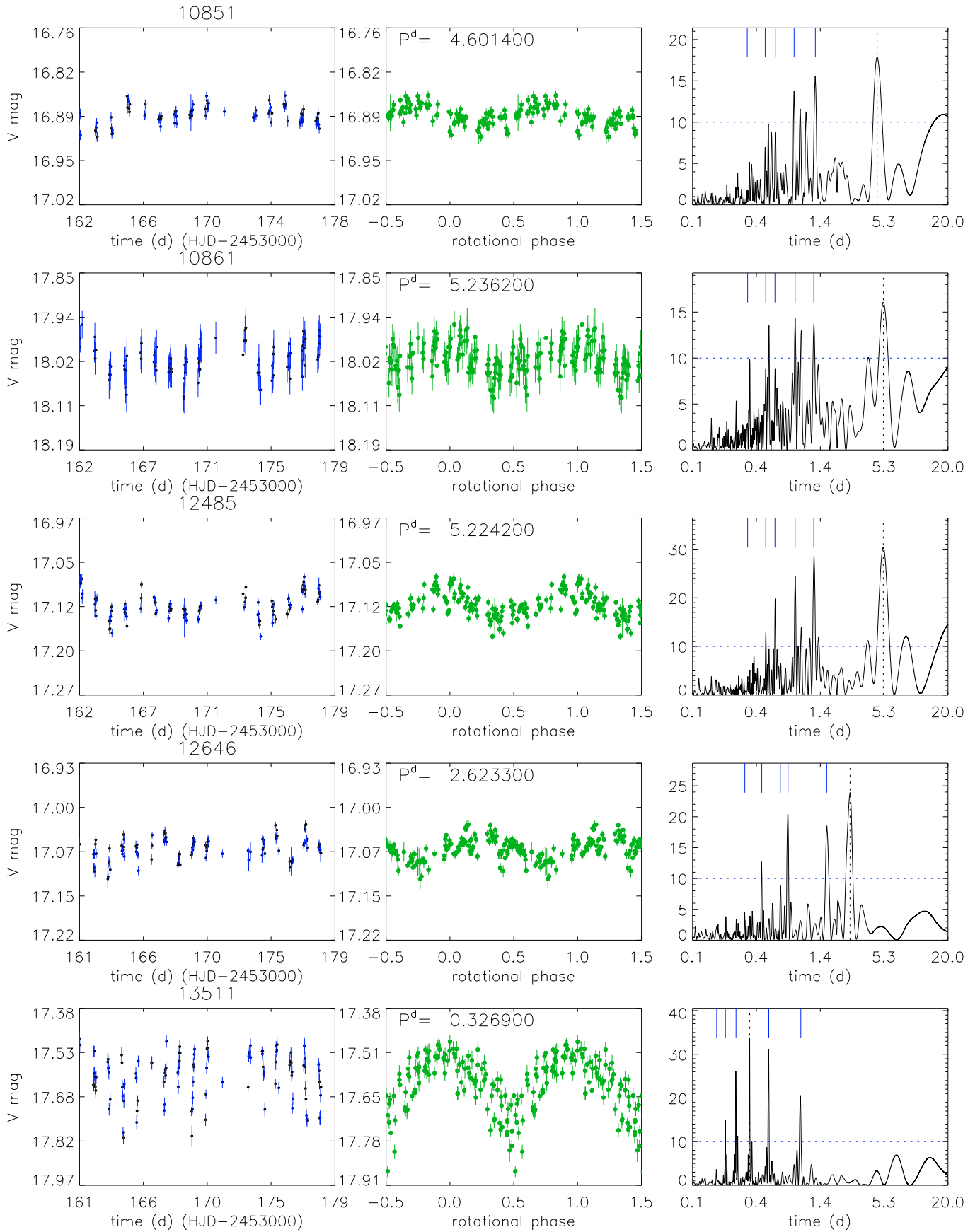


Fig. 13. As in Fig. 12.

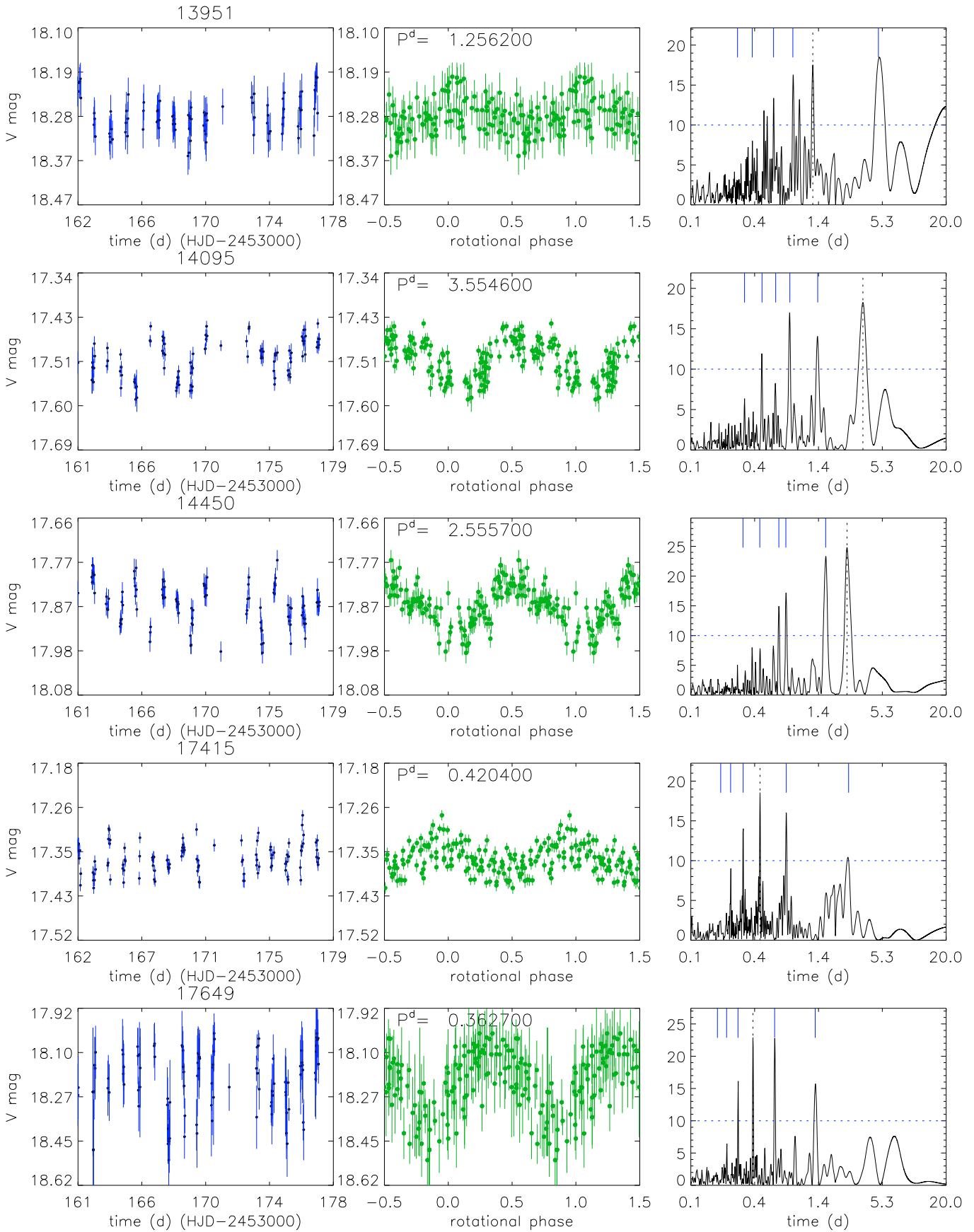


Fig. 14. As in Fig. 12.

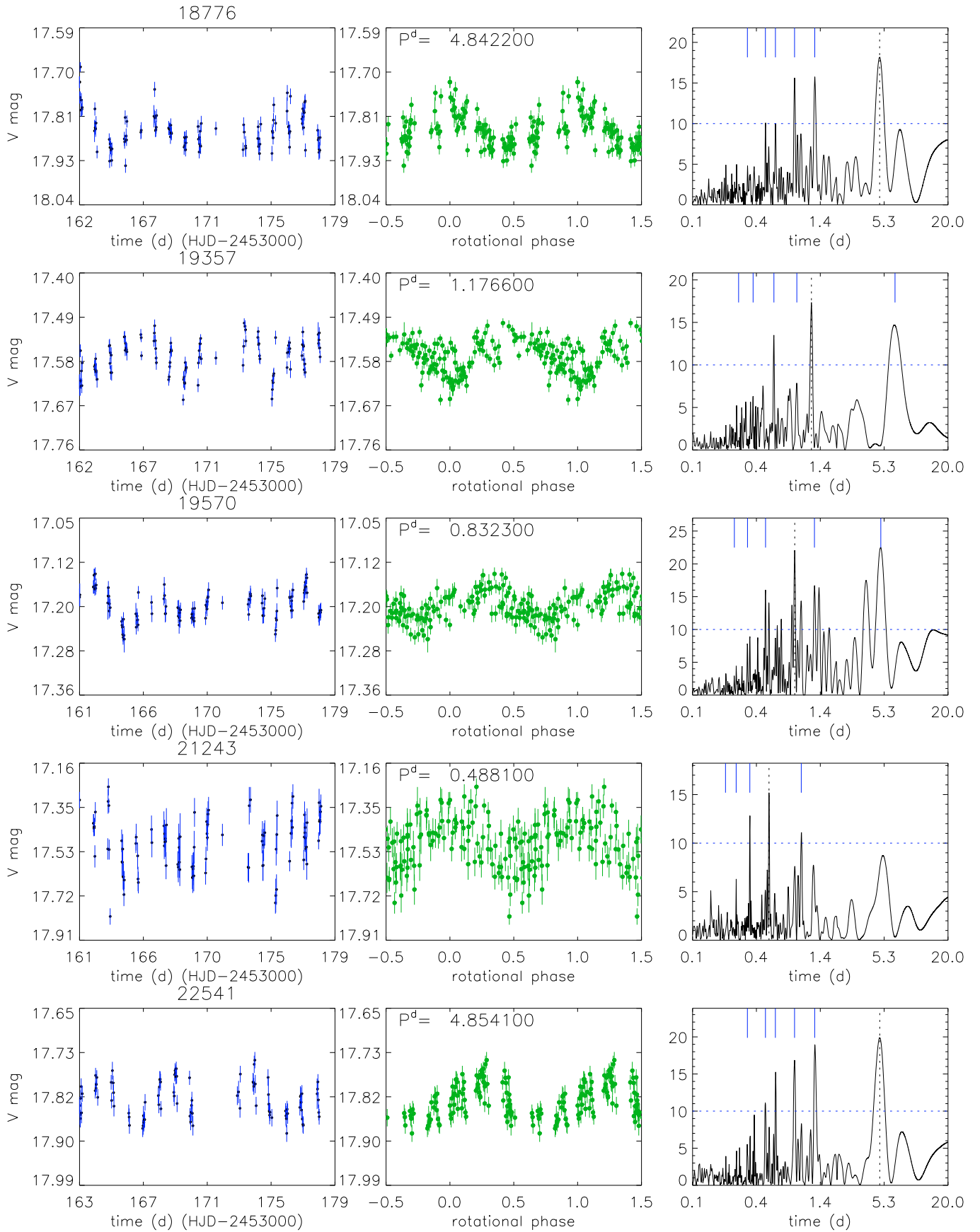


Fig. 15. As in Fig. 12.

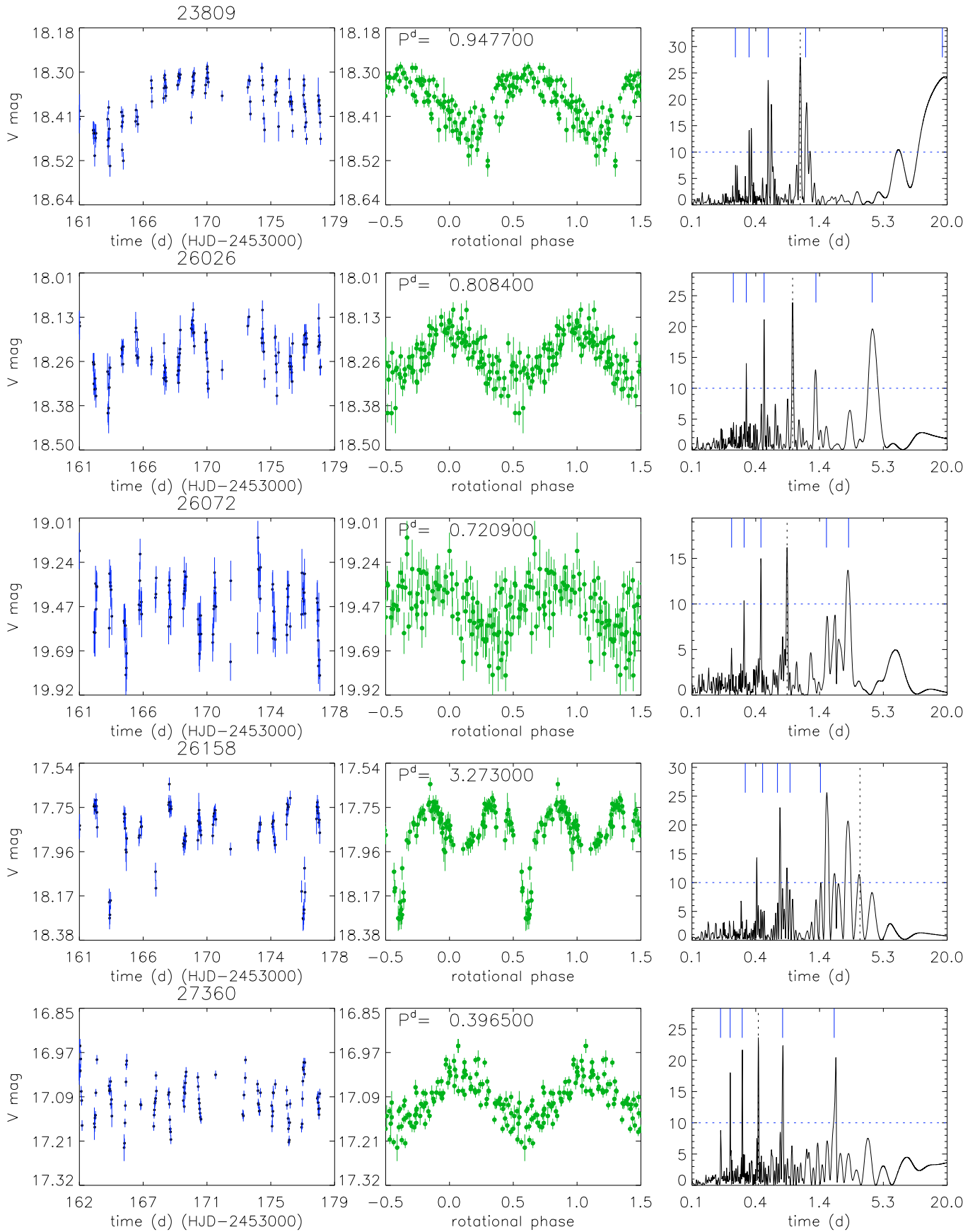


Fig. 16. As in Fig. 12.

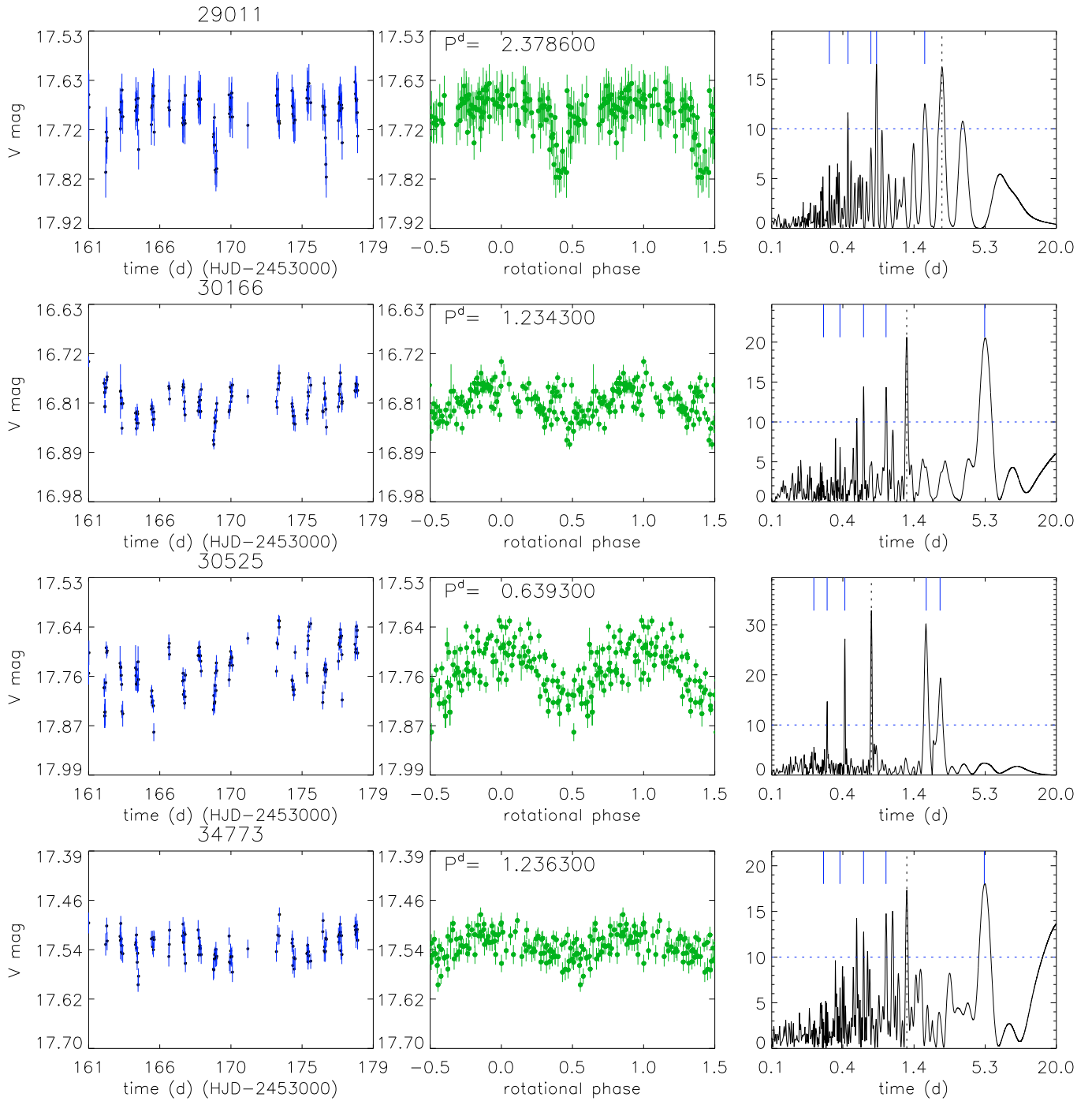


Fig. 17. As in Fig. 12.

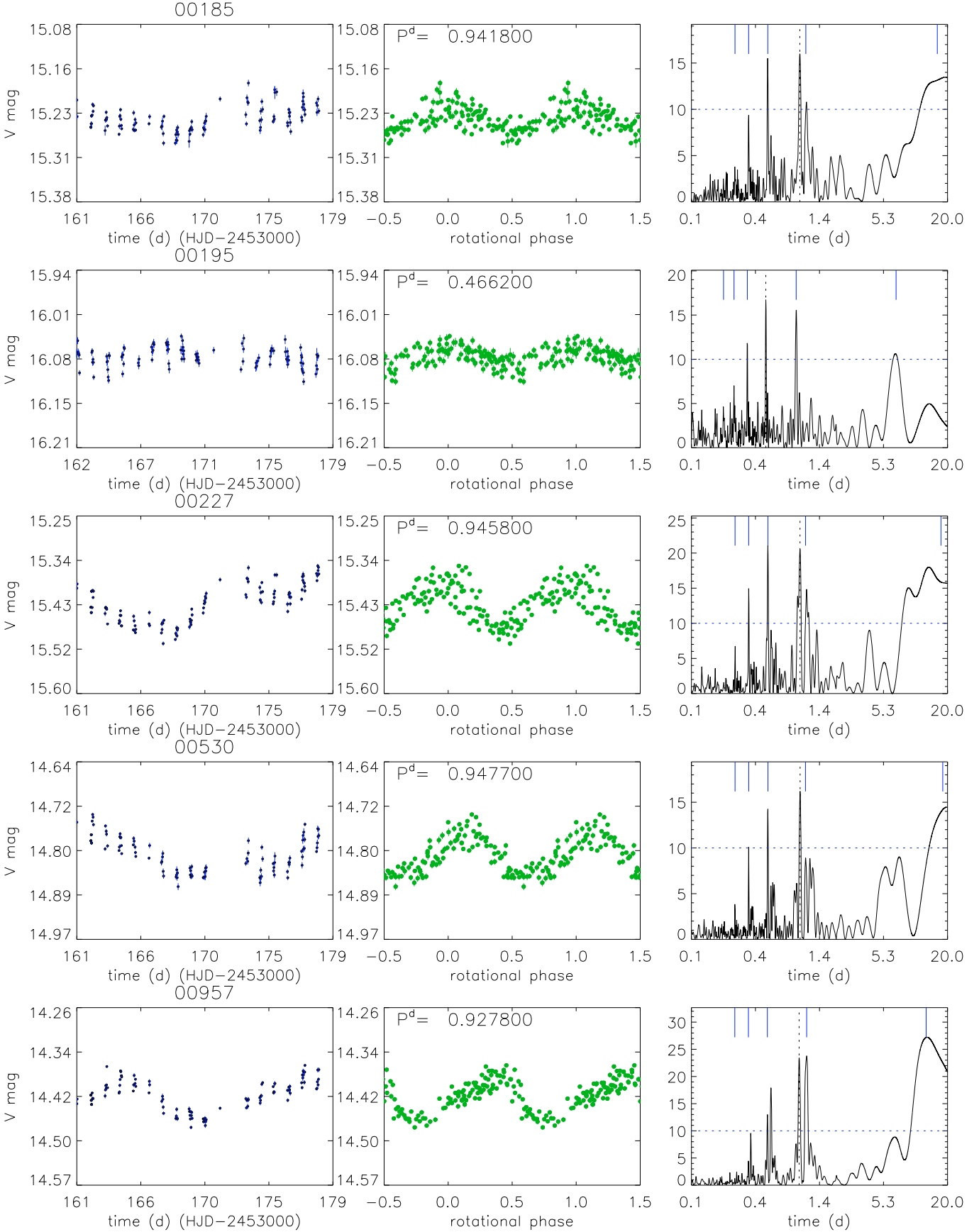


Fig. 18. Periodic cluster non-members discovered in the FoV of M 11. *From left panel:* V-band time series, phased light curve, and Scargle periodogram. See Sect. 4 for a detailed description.

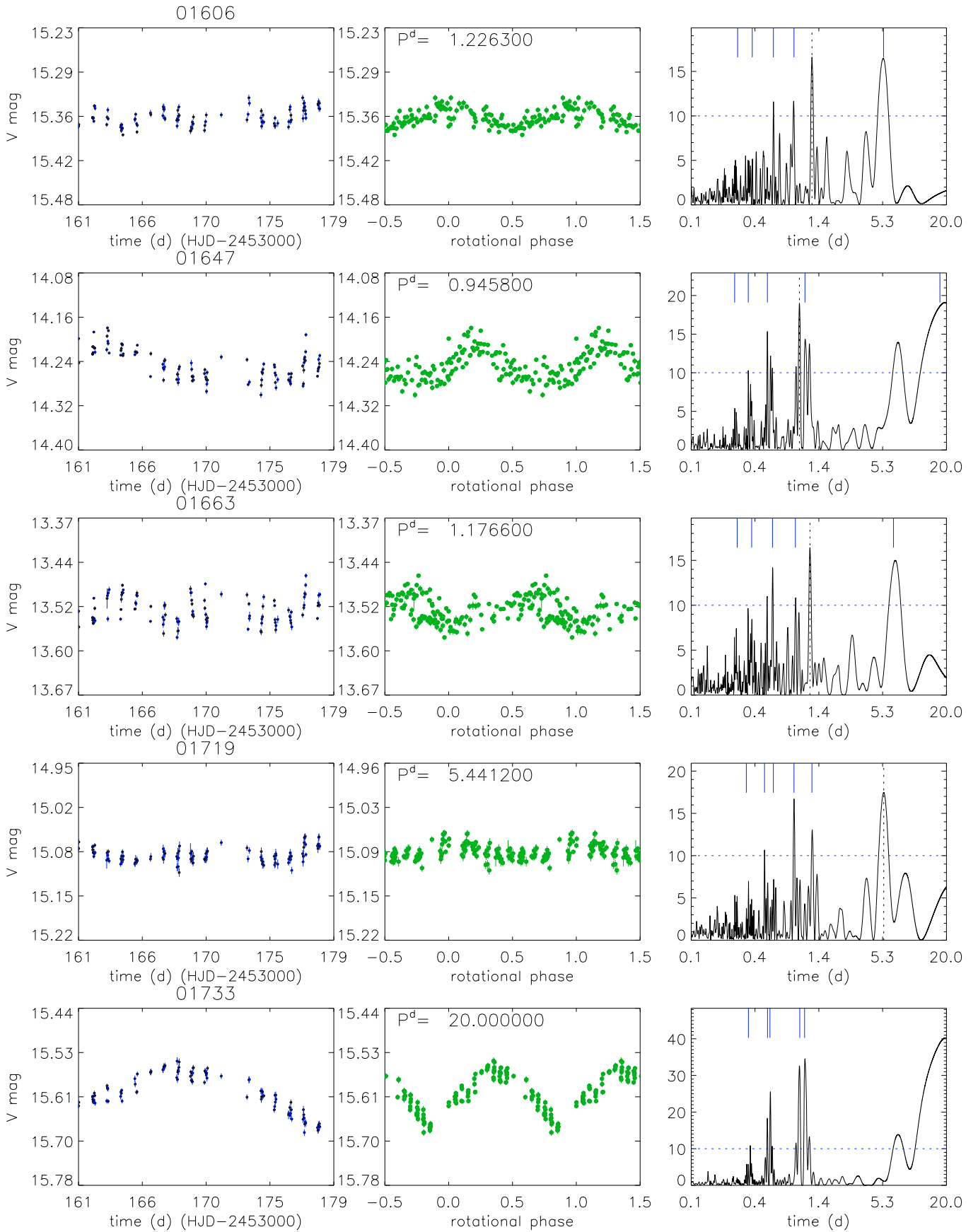


Fig. 19. As in Fig. 18.

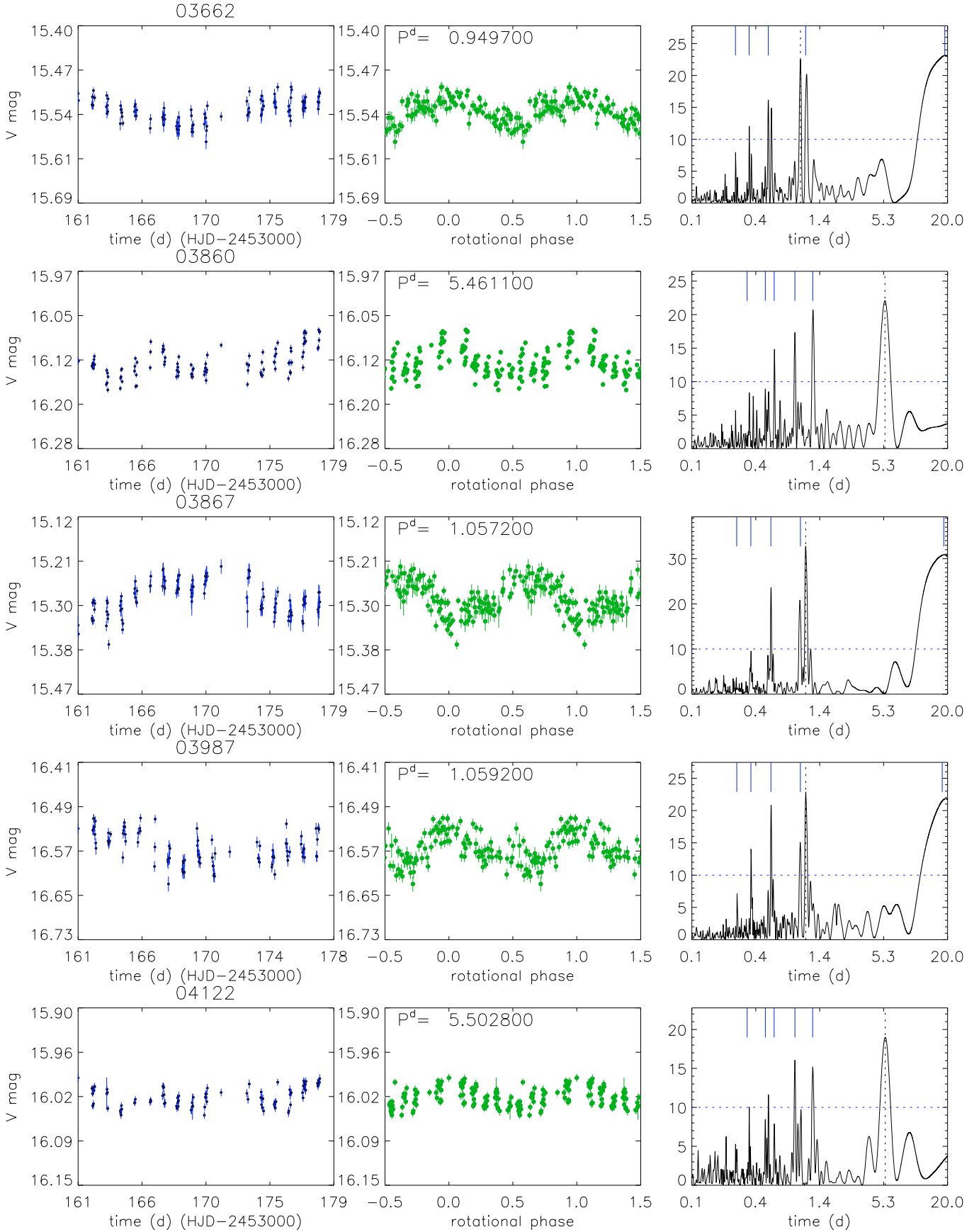


Fig. 20. As in Fig. 18.

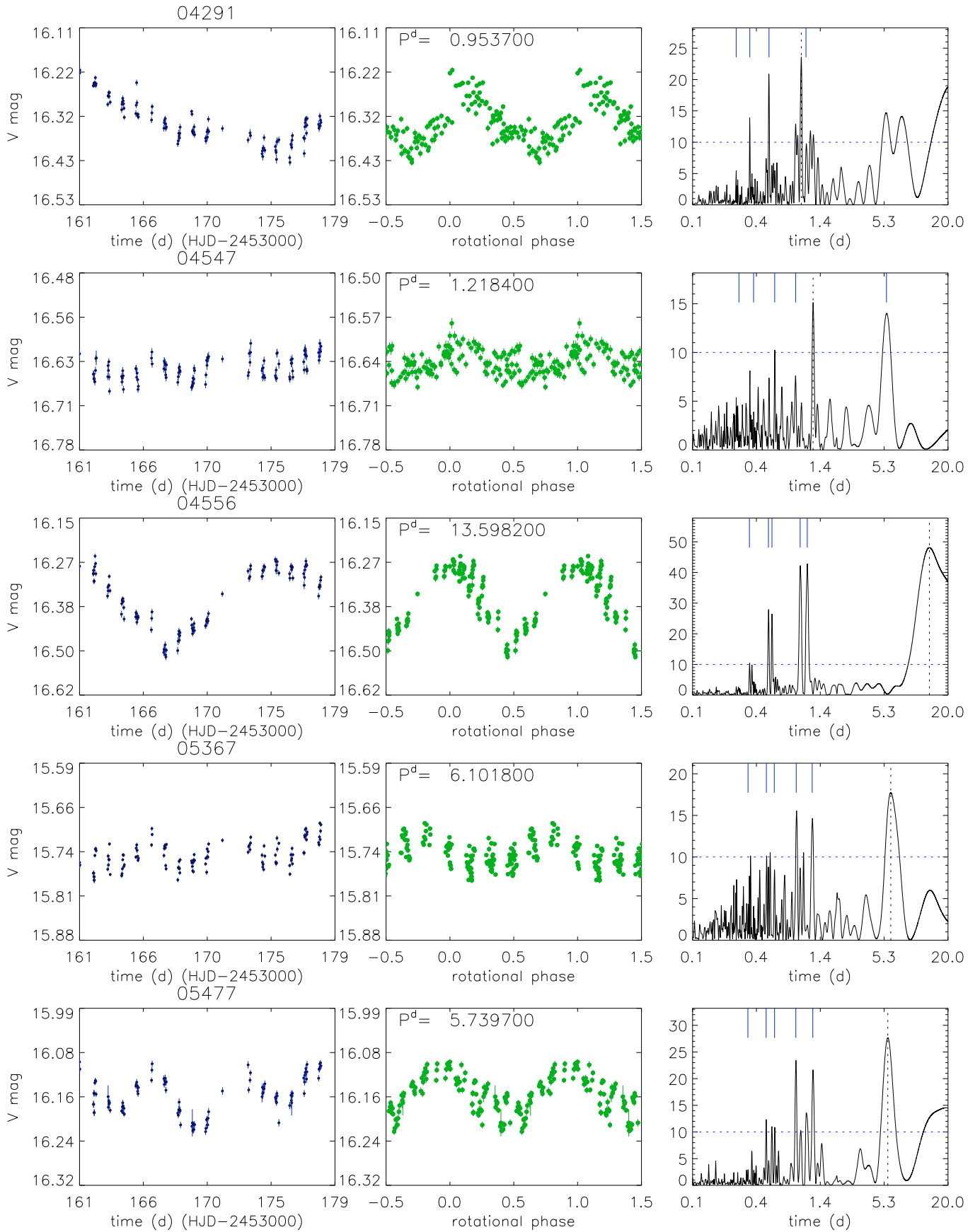


Fig. 21. As in Fig. 18.

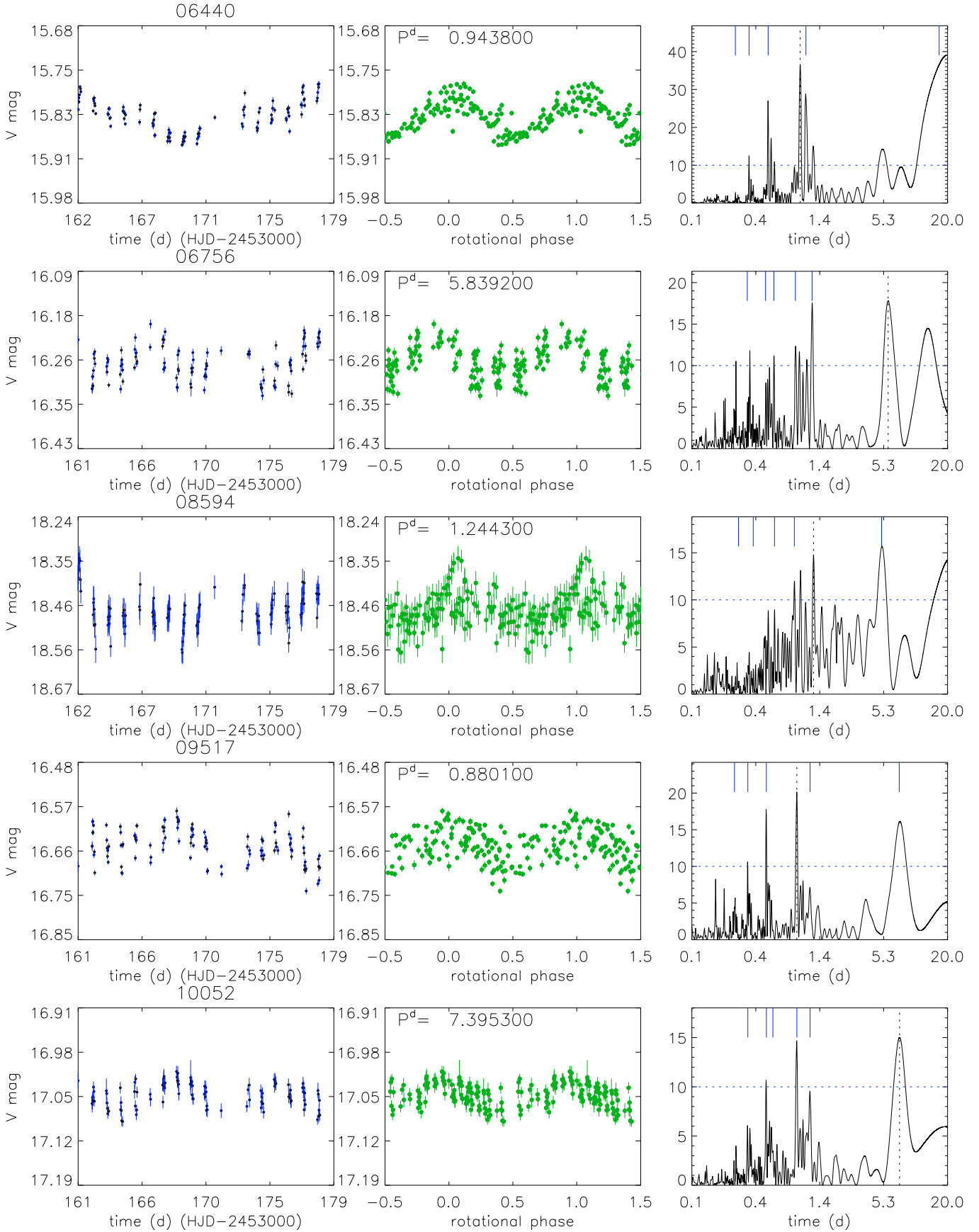


Fig. 22. As in Fig. 18.

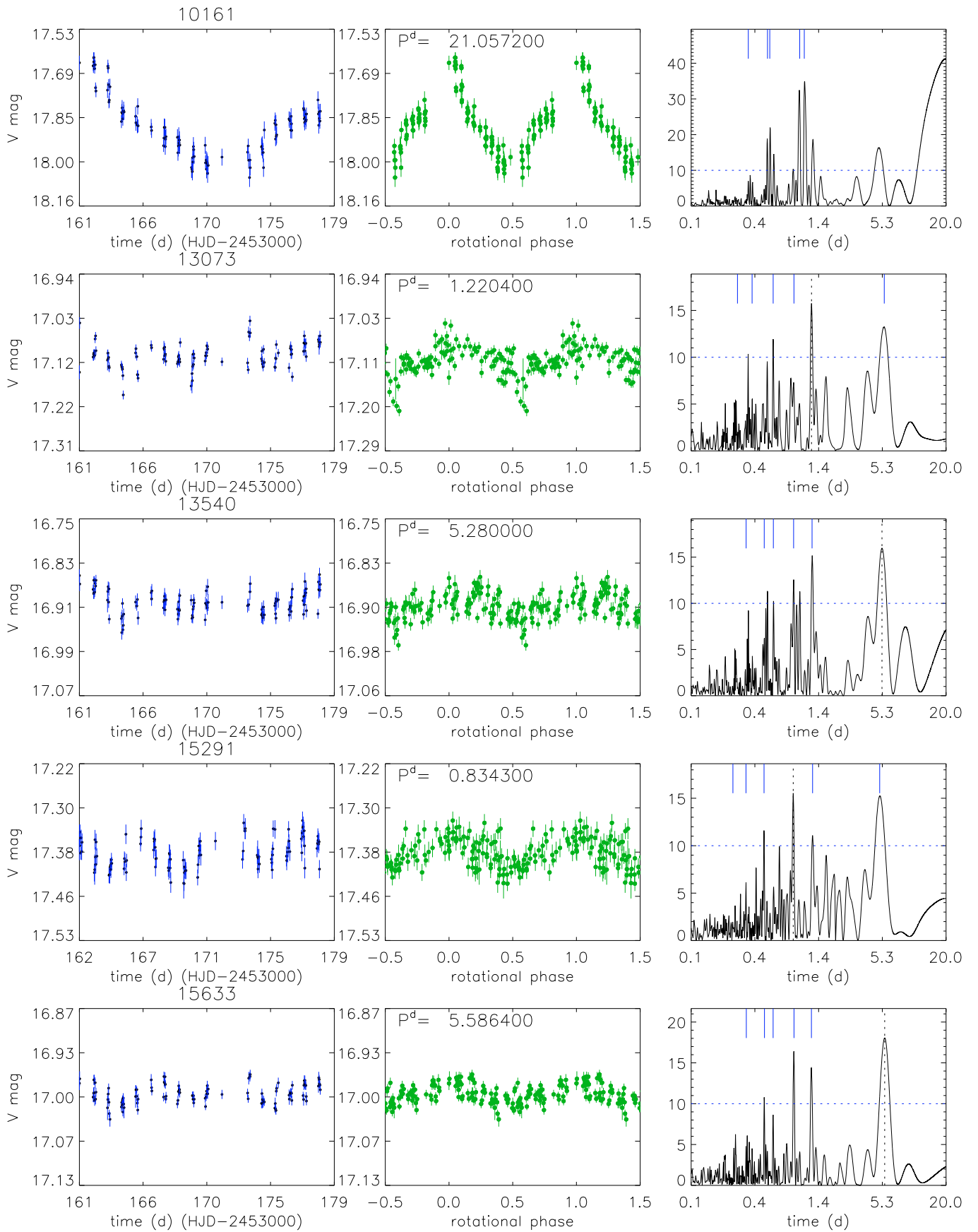


Fig. 23. As in Fig. 18.

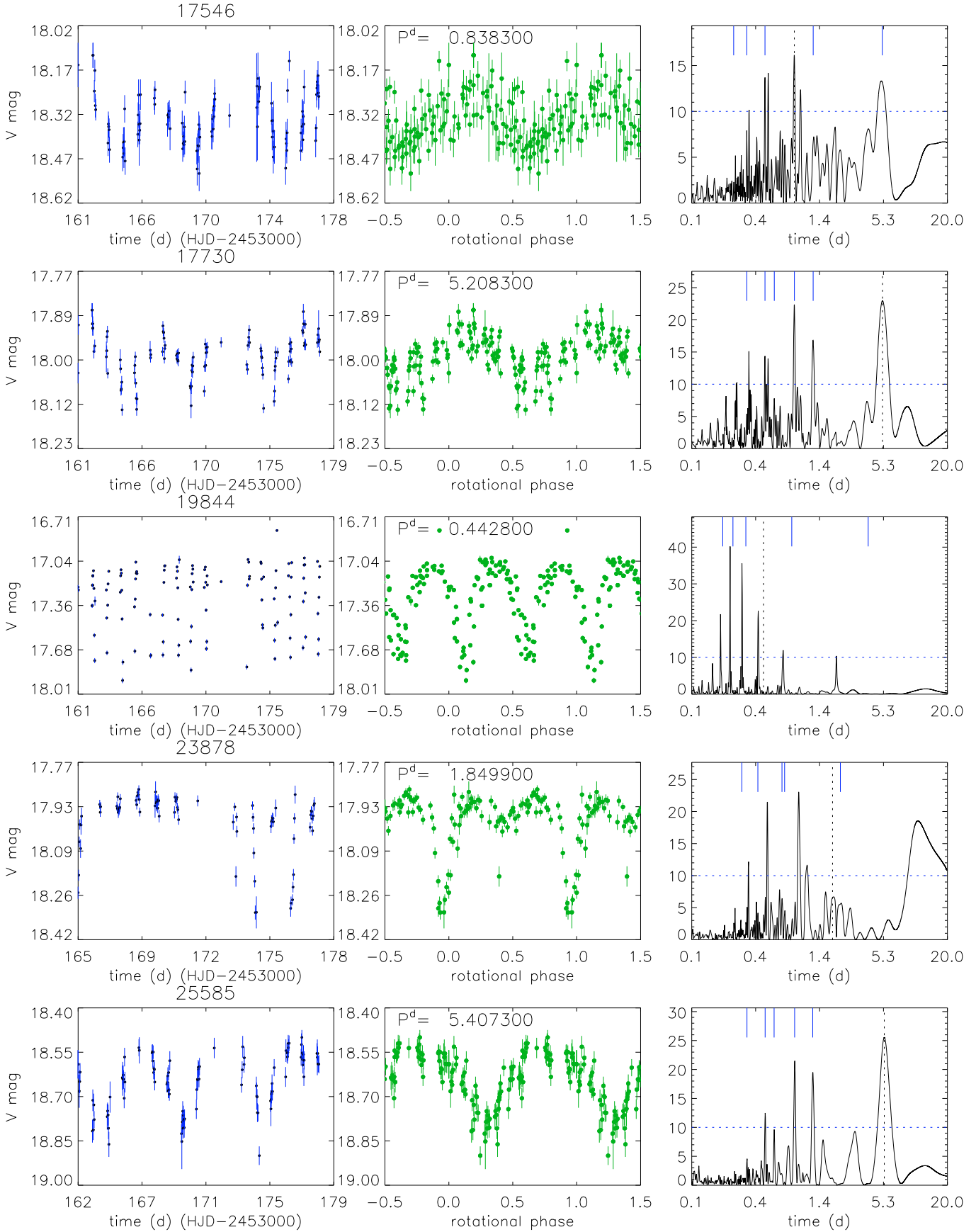


Fig. 24. As in Fig. 18.

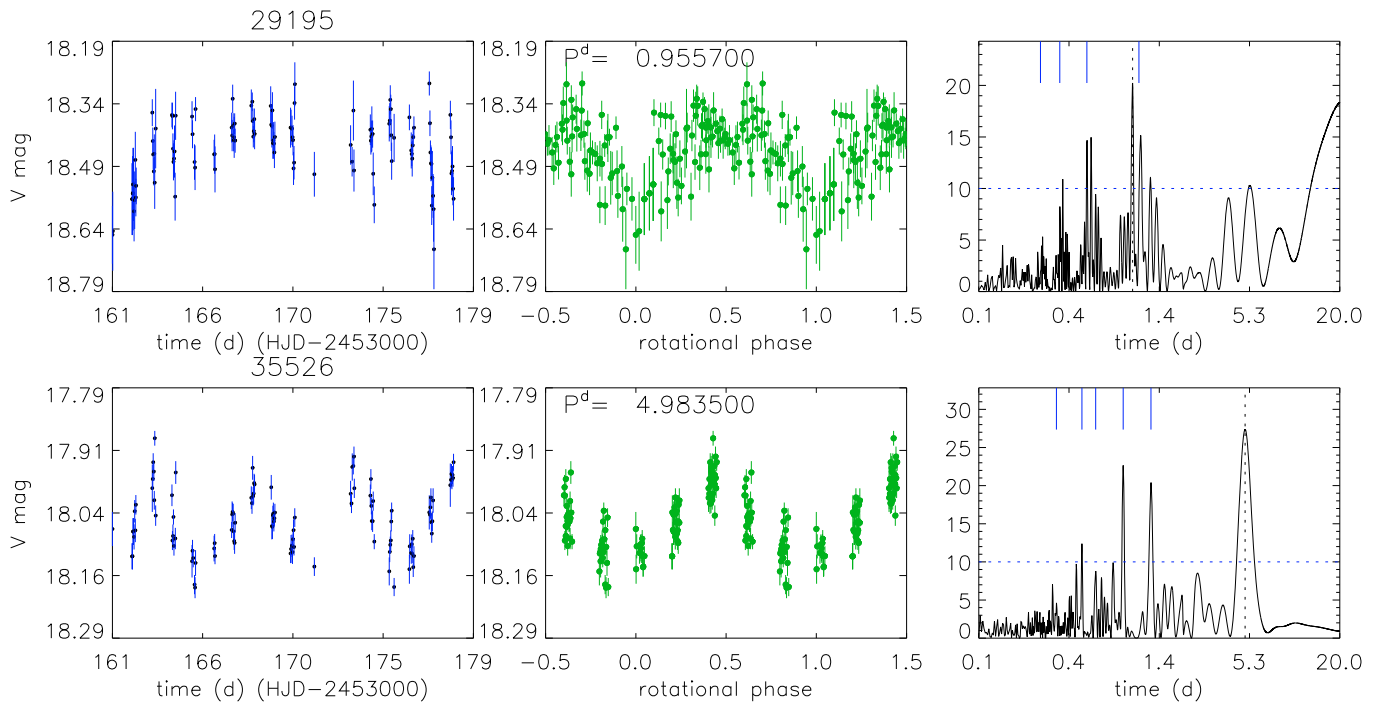


Fig. 25. As in Fig. 18.